PHYSICAL REVIEW A VOLUME 25, NUMBER 5 MAY 1982

Comparison between dressed-atom and bare-atom pictures in laser spectroscopy

P. R. Berman and Rainer Salomaa*
Physics Department, New York University, 4 Washington Place, New York, New York 10003

(Received 26 August 1981)

The theory of the interaction between radiation fields and atoms as applied to laser spectroscopy can be approached using either a bare-atom picture (BAP) or dressed-atom picture (DAP). In the BAP, the basis states are those of the free atoms and free field while, in the DAP, the basis states encompass some part of the atom-field interaction. The theory of saturation spectroscopy in three-level systems is discussed using both approaches. Whereas calculations are usually more easily done using the BAP, one can gain useful insight into the underlying physical processes from the DAP. Moreover, when the radiation field strengths (in frequency units) are larger than the relaxation rates in the problem, the DAP equations simplify considerably and lead to line-shape expressions which may be given a simple interpretation. The DAP is used to obtain resonance conditions for traveling-wave fields interacting with three- and four-level atoms and for a standing-wave saturator and traveling-wave probe interacting with a three-level atom. In addition, the DAP is applied to several problems involving optical coherent transients. A comparison is made between the various advantages of the BAP and DAP and an interesting duality between the two approaches is noted.

I. INTRODUCTION

There exists today a wide variety of "Doppler-free" methods for obtaining absorption spectra associated with atomic or molecular transitions.[1-6] The methods are "Doppler free" in that the width normally occurring in linear spectroscopy can be substantially reduced or totally eliminated using nonlinear techniques. This suppression of the Doppler width is generally achieved in one of two ways. First, one can limit those atoms participating in the absorption process to a narrow velocity range (either by use of an atomic beam or by selective excitation with a laser field) leading to a corresponding reduction of the Doppler width. Alternatively, one can arrange for the atoms to interact with two fields such that the resultant frequency seen in the atomic frame is not strongly dependent on velocity (cancellation of Doppler phases). Coherent transient spectroscopy provides another method for obtaining spectral information that is essentially free of the Doppler width. It is also possible to combine the various methods.

There exists a rich literature devoted to the theory of nonlinear saturation spectroscopy.[1-25] The approaches can be divided into roughly three groups. First, there is the so-called bare-atom picture (BAP) in which the atom-field interactions are represented in terms of a basis using the (bare) atomic eigenstates.[7-18] Second, there is the dressed-atom picture (DAP) in which all or part of the atom-field interaction is solved exactly and the resultant atom-field eigenstates are used as the basis for further calculations.[12,19-24] Finally there are resolvent methods which will not be discussed here.[25]

Most calculations were originally performed using the BAP. For two- or three-level atomic systems interacting with two or more radiation fields, the "Doppler-free" absorption spectra were calculated using a density-matrix approach. It soon became appreciated, however, that the DAP approach, previously used to describe optical pumping experiments,[26] could be advantageously applied to laser spectroscopy experiments when one or more of the fields is intense. The dressed-atom approach has proven to be extremely useful in obtaining theoretical expressions for resonance fluorescence spectra when the exciting field is intense.[19,27]

It is the purpose of this paper to provide a comparison of the DAP and BAP, to indicate the relative advantages of each approach, and to apply the

©1982 The American Physical Society

DAP to some cases not previously considered. It is shown that the BAP equations are invariably easier to solve than the corresponding DAP ones as long as one is dealing with single-mode fields interacting with two- or three-level atomic systems. For multilevel atoms or multimode fields, both methods lead to equations that present considerable analytical difficulties.

Although the DAP equations may not provide any analytical simplifications, they do enable one to obtain an interpretation of the ongoing physical processes that may be helpful in understanding the atom-field interactions. When the frequency separation of the dressed-energy states is much greater than the relaxation rates in the problem, an important simplification occurs in the DAP. One can interpret multiphoton interactions of the BAP in terms of noninterfering single-photon transitions in the DAP. The positions (but not necessarily the strengths and widths) of the various atom-field resonances are then easily and naturally predicted using the DAP.

A comparison of the BAP and the DAP also offers an interesting duality between the two approaches. It is shown that the roles played by the atom-field coupling constants and the relaxation rates are interchanged in the BAP and DAP approaches. In coherent transient spectroscopy, what appears as an optical nutation signal in the BAP now appears as a free-induction decay in the DAP. Other features of the two approaches are discussed as applied to three-level spectroscopy, four-level spectroscopy, saturation spectroscopy involving multimode fields, and coherent transient spectroscopy.

It should be stressed that the DAP discussed in this work differs in spirit from that of conventional theories.[19–22,26] In the conventional DAP, the electromagnetic field is quantized and the dressed states are eigenstates of the atom plus field; consequently, these dressed states represent linear combinations of products of atomic and quantized-field eigenstates. In our case, the field is taken to be classical. However, by using a field-interaction representation for the various state amplitudes and forming appropriate linear combinations of the atomic-state eigenstates, one arrives at equations that are mathematically equivalent to the conventional dressed-atom ones, provided the field strengths are large enough to be treated classically. Thus, even though the DAP eigenstates using classical and quantized fields differ in a fundamental way, the conclusions and interpretations using both approaches may be similar. It is in this sense that we refer to a "dressed-atom" picture, although our dressed states are not the conventional ones appearing in quantized-field treatments.[19–22,26]

In Sec. II the basic formalism is described and a comparison between the BAP and DAP is given in Sec. III. The DAP is applied to the saturation spectroscopy of homogeneously and inhomogeneously broadened three-level atoms in Secs. IV and V, respectively. In Sec. VI, we discuss the manner in which the DAP can be applied to multilevel atoms or multimode fields and in Sec. VII, coherent transient effects are discussed using the DAP. Some conclusions concerning the relative merits of the two approaches are given in Sec. VIII.

Much of the material presented in Secs. II–V is not new, but is reassembled there to provide the basis for a comparison between the BAP and DAP and to lay the foundation for the material that follows.

II. GENERAL FORMALISM

We consider an idealized three-level moving atom which interacts with a linearly polarized electromagnetic field of the form

$$\vec{E}(z,t)=\hat{e}_x[E_1\cos(\Omega_1 t-K_1 z+\varphi_1)+E_2\cos(\Omega_2 t-K_2 z+\varphi_2)]\ . \tag{2.1}$$

The atom-field interaction is of the form $\mu_x E(z,t)$ where $-\mu_x$ is the x component of the atomic dipole operator. It is assumed that the wave (E_1,Ω_1) couples the atomic states $|1\rangle$ and $|2\rangle$ only and (E_2,Ω_2) the states $|2\rangle$ and $|3\rangle$ only. Within the rotating-wave approximation,[28] the reduced density matrix of the atom in the field-interaction representation[29] obeys the master equation[12,19]

$$\dot{\tilde{\rho}}=(i\hbar)^{-1}[\tilde{H},\tilde{\rho}]+\dot{\tilde{\rho}}_{\text{rel}}+\Lambda\ . \tag{2.2}$$

Equation (2.2) contains three contributions. The first of these involves an effective Hamiltonian $\tilde{H}$ and represents the atom-field interaction. The matrix $\tilde{H}$ is given by

$$\tilde{H}=\hbar\begin{bmatrix}-\tilde{\Delta}_{21} & \alpha_1 & 0\\ \alpha_1 & 0 & \alpha_2\\ 0 & \alpha_2 & \tilde{\Delta}_{32}\end{bmatrix}, \tag{2.3}$$

where we have denoted the Doppler-shifted detunings by

$$\tilde{\Delta}_{21}=\Delta_{21}+k_1 v \ , \tag{2.4a}$$

$$\tilde{\Delta}_{32}=\Delta_{32}+k_2 v \ , \tag{2.4b}$$

where

$$\begin{aligned} &\Delta_{21}=\omega_{21}-\mathrm{sgn}(\omega_{21})\Omega_1 \ , \\ &\Delta_{32}=\omega_{32}-\mathrm{sgn}(\omega_{32})\Omega_2 \ , \end{aligned} \tag{2.4c}$$

$$\begin{aligned} &k_1=\mathrm{sgn}(\omega_{21})K_1 \ , \\ &k_2=\mathrm{sgn}(\omega_{32})K_2 \ , \end{aligned} \tag{2.4d}$$

and the Rabi frequencies by

$$\alpha_1=\mu_{21}E_1/2\hbar \ , \tag{2.5a}$$

$$\alpha_2=\mu_{32}E_2/2\hbar \ , \tag{2.5b}$$

in which ω_{ij} is the energy spacing (in units $\hbar$) between levels i and j, $\mu_{ij}=\mu_{ji}$ is the x component of the ij dipole matrix element (notice $\mu_{31}=0$), and v is the z component of the atomic velocity. The second term in Eq. (2.2) describes relaxation processes and is of the form[30]

$$(\dot{\tilde{\rho}}_{\mathrm{rel}})_{ij}=\sum_{k,l} R_{ij;kl}\tilde{\rho}_{kl} \ , \tag{2.6}$$

where the elements $R_{ij;kl}$ represent the effects of spontaneous emission or collisional relaxation. The spontaneous emission can lead either to decay *outside* of the three-level system or to a transfer of population between some of the levels. The final term in Eq. (2.2) is an incoherent pumping matrix whose elements are of the form

$$\Lambda_{ij}=\Lambda_i\delta_{i,j} \ . \tag{2.7}$$

The states $|1\rangle$ and $|2\rangle$ are assumed to be strongly coupled by α_1, whereas α_2 provides a weak coupling between $|2\rangle$ and $|3\rangle$. Many effects of the strong field are conveniently incorporated by transforming to a "dressed" basis defined by

$$|A\rangle=\cos\theta\,|1\rangle-\sin\theta\,|2\rangle \ , \tag{2.8a}$$

$$|B\rangle=\sin\theta\,|1\rangle+\cos\theta\,|2\rangle \ , \tag{2.8b}$$

$$|C\rangle=|3\rangle \ , \tag{2.8c}$$

with

$$\sin\theta=\{\tfrac{1}{2}[1-\tilde{\Delta}_{21}(\tilde{\Delta}_{21}^2+4\alpha_1^2)^{-1/2}]\}^{1/2} \ , \tag{2.9a}$$

$$\cos\theta=\{\tfrac{1}{2}[1+\tilde{\Delta}_{21}(\tilde{\Delta}_{21}^2+4\alpha_1^2)^{-1/2}]\}^{1/2} \ . \tag{2.9b}$$

In the discussion that follows, the states $|i\rangle$ ($i=1,2,3$), will be referred to as states in a bare-atom picture (BAP) and the states $|\alpha\rangle$ ($\alpha=A,B,C$), will be referred to as states in a dressed-atom picture (DAP).

The transformation (2.8) may be written

$$|\alpha\rangle=T_{\alpha i}\,|i\rangle \ , \tag{2.10}$$

where the summation convention is adopted and elements $T_{\alpha i}$ are given by

$$T_{\alpha i}=(T^{-1})_{i\alpha}=\langle i\,|\,\alpha\rangle \ . \tag{2.11}$$

In terms of the T matrix the transformation between the dressed and bare density matrices is

$$\tilde{\rho}_B=T^{-1}\tilde{\rho}_D T \ , \tag{2.12}$$

which is used to transform Eq. (2.2) into

$$\dot{\tilde{\rho}}_D=(i\hbar)^{-1}[\tilde{H}_D,\tilde{\rho}_D]+\dot{\tilde{\rho}}_{D,\mathrm{rel}}+\Lambda_D \ , \tag{2.13}$$

where

$$\tilde{H}_D=T\tilde{H}_B T^{-1}=\hbar\begin{bmatrix} -\frac{1}{2}\tilde{\Delta}_{21}-\frac{1}{2}\omega_{BA} & 0 & -\alpha_2\sin\theta \\ 0 & -\frac{1}{2}\tilde{\Delta}_{21}+\frac{1}{2}\omega_{BA} & \alpha_2\cos\theta \\ -\alpha_2\sin\theta & \alpha_2\cos\theta & \tilde{\Delta}_{32} \end{bmatrix} \ , \tag{2.14}$$

$$\omega_{BA}=(\tilde{\Delta}_{21}^2+4\alpha_1^2)^{1/2} \ , \tag{2.15}$$

$$(\dot{\tilde{\rho}}_{D,\mathrm{rel}})_{\alpha\beta}=(R_D)_{\alpha\beta;\gamma\delta}(\tilde{\rho}_D)_{\gamma\delta} \ , \tag{2.16}$$

$$(R_D)_{\alpha\beta;\gamma\delta}=T_{\alpha i}T_{\beta j}T_{\gamma k}T_{\delta l}R_{ij;kl} \ , \tag{2.17}$$

$$(\Lambda_D)_{\alpha\beta}=T_{\alpha i}T_{\beta i}\Lambda_i \ . \tag{2.18}$$

[The angle θ in Eq. (2.9) is taken to lie in the range $0<\theta<\pi/2$ such that $\cos\theta$ and $\sin\theta$ are positive. With this choice, dressed state B always has a greater energy than dressed state A. In the limit that $\alpha_1 \to 0$, states $|A\rangle, |B\rangle \to |1\rangle, |2\rangle$ if $\tilde{\Delta}_{21} > 0$ and $|A\rangle, |B\rangle \to |2\rangle, |1\rangle$ if $\tilde{\Delta}_{21} < 0$.]

The transformation T has been chosen to diagonalize the $A-B$ submatrix of $\tilde{H}_D$. In the limit that $\alpha_2 \to 0$, $\tilde{H}_D$ is diagonal and one has a complete solution to the problem. The DAP will be particularly useful when α_2 is small, enabling one to carry out a perturbation expansion in this parameter. Although the matrix $\tilde{H}_D$ has a simple structure, the relaxation and pumping terms are now more complicated. The pumping matrix, which is diagonal in the BAP, has *both* diagonal and off-diagonal elements in the DAP as given in Eq. (2.18). Moreover, the relaxation terms are most naturally expressed in the BAP, where one can typically take (no sum)

$$\begin{aligned} R_{ij;kl} = & -\gamma_{ij}\delta_{i,k}\delta_{j,l}(1-\delta_{i,j}) \\ & -\Gamma_i \delta_{i,j}\delta_{i,k}\delta_{i,l} + \Gamma_{ki}\delta_{i,j}\delta_{k,l}(1-\delta_{i,k}) \end{aligned} \tag{2.19}$$

leading to a relaxational time rate of change of $\tilde{\rho}$ of the form

$$(\dot{\tilde{\rho}}_{\mathrm{rel}})_{ij} = -\gamma_{ij}\tilde{\rho}_{ij} \quad (i \neq j) , \tag{2.20}$$

$$(\dot{\tilde{\rho}}_{\mathrm{rel}})_{ii} = -\Gamma_i \tilde{\rho}_{ii} + \sum_{j(\neq i)} \Gamma_{ji}\tilde{\rho}_{jj} , \tag{2.21}$$

where Γ_i is the total decay rate of state i and Γ_{ji} describes population transfer from j to i due to spontaneous emission or collisions. While the relaxational decay and coupling in the BAP given by Eqs. (2.20) and (2.21) is fairly simple, the corresponding coupling in the DAP given by Eqs. (2.16)–(2.17) involves many more terms. Explicit expressions for the relaxation rates are given in Appendix A.

To compare the BAP and DAP we write down the equations of the components of the density-matrix elements in both representations. For simplicity, we adopt a relaxation scheme in which $\Gamma_{ij} = 0$ and $\gamma_{ij} = \frac{1}{2}(\Gamma_i + \Gamma_j)$, corresponding to the case in which each level decays to some states *other* than states 1, 2, or 3. In the BAP, one has

$$\dot{\tilde{\rho}}_{11} = \Lambda_1 - \Gamma_1\tilde{\rho}_{11} + 2\alpha_1 \operatorname{Im}(\tilde{\rho}_{21}) , \tag{2.22a}$$

$$\dot{\tilde{\rho}}_{22} = \Lambda_2 - \Gamma_2\tilde{\rho}_{22} - 2\alpha_1 \operatorname{Im}(\tilde{\rho}_{21}) + 2\alpha_2 \operatorname{Im}(\tilde{\rho}_{32}) , \tag{2.22b}$$

$$\dot{\tilde{\rho}}_{33} = \Lambda_3 - \Gamma_3\tilde{\rho}_{33} - 2\alpha_2 \operatorname{Im}(\tilde{\rho}_{32}) , \tag{2.22c}$$

$$\dot{\tilde{\rho}}_{21} = -(\gamma_{21} + i\tilde{\Delta}_{21})\tilde{\rho}_{21} + i\alpha_1(\tilde{\rho}_{22} - \tilde{\rho}_{11}) - i\alpha_2\tilde{\rho}_{31} , \tag{2.22d}$$

$$\dot{\tilde{\rho}}_{32} = -(\gamma_{32} + i\tilde{\Delta}_{32})\tilde{\rho}_{32} + i\alpha_2(\tilde{\rho}_{33} - \tilde{\rho}_{22}) + i\alpha_1\tilde{\rho}_{31} , \tag{2.22e}$$

$$\dot{\tilde{\rho}}_{31} = -(\gamma_{31} + i\tilde{\Delta}_{21} + i\tilde{\Delta}_{32})\tilde{\rho}_{31} + i\alpha_1\tilde{\rho}_{32} - i\alpha_2\tilde{\rho}_{21} , \tag{2.22f}$$

$$\tilde{\rho}_{ij} = \tilde{\rho}_{ji}{}^{*} , \tag{2.22g}$$

while in the DAP, the corresponding equations read:

$$\dot{\tilde{\rho}}_{AA} = \Lambda_A - \Gamma_A\tilde{\rho}_{AA} + 2\beta \operatorname{Re}(\tilde{\rho}_{BA}) + 2\alpha_A \operatorname{Im}(\tilde{\rho}_{CA}) , \tag{2.23a}$$

$$\dot{\tilde{\rho}}_{BB} = \Lambda_B - \Gamma_B\tilde{\rho}_{BB} + 2\beta \operatorname{Re}(\tilde{\rho}_{BA}) + 2\alpha_B \operatorname{Im}(\tilde{\rho}_{CB}) , \tag{2.23b}$$

$$\dot{\tilde{\rho}}_{CC} = \Lambda_C - \Gamma_C\tilde{\rho}_{CC} - 2\alpha_A \operatorname{Im}(\tilde{\rho}_{CA}) - 2\alpha_B \operatorname{Im}(\tilde{\rho}_{CB}) , \tag{2.23c}$$

$$\begin{aligned} \dot{\tilde{\rho}}_{CA} = & -(\gamma_{CA} + i\omega_{CA})\tilde{\rho}_{CA} + i\alpha_A(\tilde{\rho}_{CC} - \tilde{\rho}_{AA}) \\ & - i\alpha_B\tilde{\rho}_{BA} + \beta\tilde{\rho}_{CB} , \end{aligned} \tag{2.23d}$$

$$\begin{aligned} \dot{\tilde{\rho}}_{CB} = & -(\gamma_{CB} + i\omega_{CB})\tilde{\rho}_{CB} + i\alpha_B(\tilde{\rho}_{CC} - \tilde{\rho}_{BB}) \\ & - i\alpha_A\tilde{\rho}_{AB} + \beta\tilde{\rho}_{CA} , \end{aligned} \tag{2.23e}$$

$$\begin{aligned} \dot{\tilde{\rho}}_{BA} = & \Lambda_{BA} - (\gamma_{BA} + i\omega_{BA})\tilde{\rho}_{BA} + \beta(\tilde{\rho}_{AA} + \tilde{\rho}_{BB}) \\ & + i\alpha_A\tilde{\rho}_{BC} - i\alpha_B\tilde{\rho}_{CA} , \end{aligned} \tag{2.23f}$$

$$\tilde{\rho}_{\alpha\beta} = \tilde{\rho}_{\beta\alpha}{}^{*} , \tag{2.23g}$$

where

$$\Lambda_A = \Lambda_1 \cos^2\theta + \Lambda_2 \sin^2\theta , \tag{2.24a}$$

$$\Lambda_B = \Lambda_1 \sin^2\theta + \Lambda_2 \cos^2\theta , \tag{2.24b}$$

$$\Lambda_C = \Lambda_3 , \tag{2.24c}$$

$$\Lambda_{BA} = \Lambda_{AB} = \tfrac{1}{2}(\Lambda_1 - \Lambda_2)\sin 2\theta , \tag{2.24d}$$

$$\Gamma_A = \Gamma_1 \cos^2\theta + \Gamma_2 \sin^2\theta , \tag{2.25a}$$

$$\Gamma_B = \Gamma_1 \sin^2\theta + \Gamma_2 \cos^2\theta , \tag{2.25b}$$

$$\Gamma_C = \Gamma_3 , \tag{2.25c}$$

$$\gamma_{\alpha\beta} = \tfrac{1}{2}(\Gamma_\alpha + \Gamma_\beta) , \tag{2.25d}$$

$$\alpha_A = -\alpha_2 \sin\theta , \tag{2.26a}$$

$$\alpha_B = \alpha_2 \cos\theta , \tag{2.26b}$$

$$\beta = \tfrac{1}{4}(\Gamma_2 - \Gamma_1)\sin 2\theta , \tag{2.27}$$

$$\omega_{CA} = \tilde{\Delta}_{32} + \tfrac{1}{2}\tilde{\Delta}_{21} + \tfrac{1}{2}(\tilde{\Delta}_{21}^2 + 4\alpha_1^2)^{1/2} , \tag{2.28a}$$

$$\omega_{CB} = \tilde{\Delta}_{32} + \tfrac{1}{2}\tilde{\Delta}_{21} - \tfrac{1}{2}(\tilde{\Delta}_{21}^2 + 4\alpha_1^2)^{1/2} . \tag{2.28b}$$

The physical observables are the populations $\tilde{\rho}_{ii}$ and terms proportional to either $\mathrm{Re}(\tilde{\rho}_{ij})$ or $\mathrm{Im}(\tilde{\rho}_{ij})$ giving the dispersion or absorption, respectively, for the saturator $(i,j=2,1)$ or probe $(i,j=3,2)$. Using Eqs. (2.8)−(2.12), one can express these BAP elements in terms of the DAP elements $\tilde{\rho}_{\alpha\beta}$ by

$$\tilde{\rho}_{11}=\cos^2\theta\,\tilde{\rho}_{AA}+\sin^2\theta\,\tilde{\rho}_{BB}+\sin2\theta\,\mathrm{Re}(\tilde{\rho}_{BA})\,, \tag{2.29a}$$

$$\tilde{\rho}_{22}=\sin^2\theta\,\tilde{\rho}_{AA}+\cos^2\theta\,\tilde{\rho}_{BB}-\sin2\theta\,\mathrm{Re}(\tilde{\rho}_{BA})\,, \tag{2.29b}$$

$$\tilde{\rho}_{33}=\tilde{\rho}_{CC}\,, \tag{2.29c}$$

$$\tilde{\rho}_{21}=\tfrac{1}{2}\sin2\theta(\tilde{\rho}_{BB}-\tilde{\rho}_{AA})+\cos^2\theta\,\tilde{\rho}_{BA}-\sin^2\theta\,\tilde{\rho}_{AB}\,, \tag{2.29d}$$

$$\tilde{\rho}_{32}=\cos\theta\,\tilde{\rho}_{CB}-\sin\theta\,\tilde{\rho}_{CA}\,. \tag{2.29e}$$

It might be noted that the above equations, together with the quantum regression theorem, could also be used to calculate the spectrum of resonance fluorescence from these levels.[12,19,31]

III. COMPARISON BETWEEN BAP AND DAP: APPROXIMATE SOLUTIONS

The DAP equations are more complicated than the corresponding BAP equations, even for the simplified relaxation scheme adopted in Sec. II. One may, in particular, note the following features:

(i) In the DAP, in contrast to the BAP, the off-diagonal element $\tilde{\rho}_{BA}$ has a source term Λ_{BA}. This disappears only when $\Lambda_1=\Lambda_2$ or $\alpha_1\to0$.

(ii) All direct coupling between $\tilde{\rho}_{AA}$, $\tilde{\rho}_{AB}$, $\tilde{\rho}_{BA}$, $\tilde{\rho}_{BB}$ is proportional to the difference between the relaxation rates Γ_1 and Γ_2. The coupling parameter is of order β given in Eq. (2.27).

(iii) If we neglect Λ_{AB} and β, the DAP and BAP equations are equivalent with the replacements $\alpha_A\leftrightarrow\alpha_1$, $\alpha_B\leftrightarrow\alpha_2$, and $A,B,C\leftrightarrow1,3,2$. The prominent difference between the two representations is that, in the DAP, all couplings are of order α_2 (weak), whereas in the BAP, states 1 and 2 are strongly coupled by α_1. These features are illustrated in Fig. 1.

Clearly the BAP equations are easier to solve than those of the DAP. However, for a strong saturator, there are definite advantages in using the DAP. Moreover, the simple model configuration considered here partly hides the power of DAP. A better comparison could, perhaps, be obtained by studying a case where both pictures must be solved approximately. Some applications along these lines are presented in Secs. VI and VII. For the present, we consider the three-level scheme of Fig. 1 since it allows for comparison with well-known results.[1–25]

Regardless of the level structure, the DAP simplifies the interpretation of the probe-absorption spectrum when the saturating field is intense. As an example, consider a three-level system for which two peaks appear in the probe-absorption spectrum at $\tilde{\Delta}_{32}\simeq0$ and $\tilde{\Delta}_{32}\simeq-\tilde{\Delta}_{21}$. If α_1 is weak these resonances can be labeled as stepwise and two photon in the BAP, but this interpretation breaks down if α_1 cannot be treated in lowest-order perturbation theory. In the limit of large α_1, however, the DAP allows one to interpret the two peaks as single-photon transitions between the dressed states A-C and B-C.

One way to solve the density-matrix equations approximately is based on the assumption that the off-diagonal components are small. In the BAP this leads to ordinary perturbation solutions in powers of α_1. The expansion converges rapidly provided that $|\tilde{\Delta}_{21}|$ or the relaxation constants are much larger than α_1. In the DAP, the role of the γ's and α_1 is interchanged; therefore, the corresponding approximate solution holds in the limit that $|\tilde{\Delta}_{21}|$ or α_1 is much larger than the relaxation rates. Thus, for strong fields α_1, a perturbative approach works well in the DAP but not at all in the BAP.

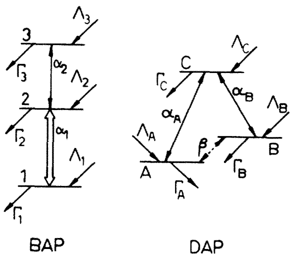

FIG. 1. A three-level system in both the BAP and DAP. In the BAP, there is incoherent pumping to and decay from each of the states. Levels 1 and 2 are coupled by a strong field α_1 and levels 2 and 3 by a weak probe field α_2. In the DAP, both couplings α_A and α_B between the dressed states are weak. However, there is now a collisional coupling β of states A and B as well as a "coherent pumping" Λ_{AB} which is not present in the BAP.

For the present, we assume (validity conditions to be stated below) that $\tilde{\rho}_{BA}$ is negligible. Then, to zeroth order in α_2 it follows immediately that the steady-state solutions to Eq. (2.23) are

$$\tilde{\rho}^0_{\alpha\beta}=(\Lambda_\alpha/\Gamma_\alpha)\delta_{\alpha,\beta}=n^0_\alpha\delta_{\alpha,\beta}\,. \tag{3.1}$$

Using Eqs. (2.23) and (2.29) one obtains

$$\tilde{\rho}_{32}=\frac{i\alpha_2\cos^2\theta(n^0_C-n^0_B)}{\gamma_{CB}+i\omega_{CB}}+\frac{i\alpha_2\sin^2\theta(n^0_C-n^0_A)}{\gamma_{CA}+i\omega_{CA}}\,. \tag{3.2}$$

The steady-state value of $\tilde{\rho}_{32}$, is related to the probe-induced polarization. It can be seen in Eq. (3.2) that the probe-field polarization may be viewed as originating from two noninteracting single-photon transitions between the dressed states C-B (corresponding strength $\alpha_2\cos^2\theta$) and C-A (strength $\alpha_2\sin^2\theta$).

An exact solution for $\tilde{\rho}_{32}$ (to first order in α_2) is given in Appendix B where it is shown that Eq. (3.2) is valid provided that both

$$(\tilde{\Delta}^2_{21}+4\alpha_1^2)^{1/2}>>\tfrac{1}{2}\,|\,\Gamma_2-\Gamma_1\,| \tag{3.3a}$$

and

$$|\,n^0_C-n^0_B\,|\cos^2\theta\,,$$

$$|\,n^0_C-n^0_A\,|\sin^2\theta>>\tfrac{1}{4}\frac{|\,\Lambda_1-\Lambda_2\,|}{\omega_{BA}}\sin^2 2\theta\,. \tag{3.3b}$$

Roughly speaking, Eqs. (3.3) are satisfied if the decay rates are much less than the frequency separation ω_{BA} between states A and B.

The widths γ_{CA}, γ_{CB} and the positions $\omega_{CB}=0$, $\omega_{CA}=0$ of the resonances given in Eq. (3.2) are accurate if (3.3a) is satisfied. Equation (3.3a) enables one to ignore any interference effects between the two single-photon transitions of the DAP. Mathematically, this assumption involves the neglect of the $\beta\tilde{\rho}_{CB}$ and $\beta\tilde{\rho}_{CA}$ terms in Eqs. (2.23d) and (2.23e), respectively, which, in turn, implies that $\tilde{\rho}_{CA}$ and $\tilde{\rho}_{CB}$ are decoupled. Equation (3.3b), on the other hand, is the requirement that terms involving $\tilde{\rho}_{BA}$ in Eqs. (2.23d)–(2.23e) are small enough to be neglected. Roughly speaking Eq. (3.3b) is valid when $(\Gamma_1+\Gamma_2)/\omega_{BA}<<1$. This condition is not sufficient if two of the dressed-state populations are equal. In this case one of the resonances in Eq. (3.2) disappears, whereas in the exact solution, the resonance does not totally vanish but is down in magnitude by a factor of order Γ/ω_{BA}.

IV. HOMOGENEOUSLY BROADENED SYSTEMS

We consider first a homogeneously broadened system in which all the detunings $\tilde{\Delta}_{ij}$ are independent of v as may be the case when laser beams interact with an atomic beam such that $\vec{k}\cdot\vec{v}=0$. Once Eq. (3.2) is valid the interpretation of the probe-absorption spectrum is extremely simple. We define the probe-absorption spectrum $I(\Delta_{32})$ as[32]

$$I(\Delta_{32})=\frac{1}{\alpha_2}\,\mathrm{Im}\{\tilde{\rho}_{32}\}\,, \tag{4.1}$$

which is obtained by combining Eqs. (4.1) and (3.2) to give

$$I(\Delta_{32})=\frac{\gamma_{CB}\cos^2\theta(n^0_C-n^0_B)}{\gamma^2_{CB}+\omega^2_{CB}}+\frac{\gamma_{CA}\sin^2\theta(n^0_C-n^0_A)}{\gamma^2_{CA}+\omega^2_{CA}}\,. \tag{4.2}$$

The two resonances are Lorentzians (which may overlap) having the following properties:

C-B transition

$$\Delta_{32}=-\tfrac{1}{2}\Delta_{21}+\tfrac{1}{2}(\Delta^2_{21}+4\alpha_1^2)^{1/2}\ \ \text{(position)}\,,$$

$$\gamma_{CB}=\gamma_{31}\sin^2\theta+\gamma_{32}\cos^2\theta\ \ \text{(width)}\,,$$

$$\cos^2\theta(n^0_C-n^0_B)/\gamma_{CB}\ \ \text{(height)}\,, \tag{4.3}$$

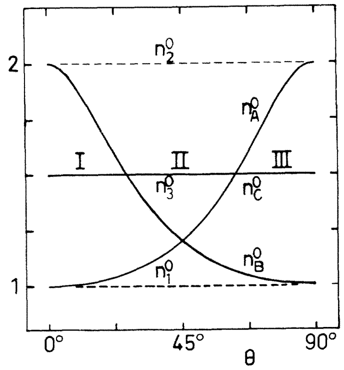

FIG. 2. Dressed-state populations n^0_A,n^0_B,n^0_C as a function of the BAP→DAP transformation angle θ. The BAP populations n^0_1, n^0_2, and $n^0_3=n^0_C$ are determined by the incoherent pumping and relaxation rates. The gain factors for the CA and CB transitions can be read directly from this graph. For the case shown ($\Gamma_1=4\Gamma_2$; $n^0_1{:}n^0_2{:}n^0_3=1{:}2{:}1.5$), region I corresponds to absorption for the CB transition and gain for CA, region II to gain for both the CA and CB transitions, and region III to gain for the CB transition and absorption for CA.

C-*A* transition

$$\Delta_{32}=-\tfrac{1}{2}\Delta_{21}-\tfrac{1}{2}(\Delta_{21}^2+4\alpha_1^2)^{1/2}\ \text{(position)}\,,$$

$$\gamma_{CA}=\gamma_{31}\cos^2\theta+\gamma_{32}\sin^2\theta\ \text{(width)}\,,$$

$$\sin^2\theta(n_C^0-n_A^0)/\gamma_{CA}\ \text{(height)}\,. \tag{4.4}$$

The dependence of the heights and the nature (i.e., absorption or stimulated emission) of the resonances on n_A^0, n_B^0, and n_C^0 is easily carried out with graphs like that shown in Fig. 2 which is constructed using Eqs. (2.24), (2.25), and (3.1). The linewidths always remain below $\max\{\gamma_{32},\gamma_{31}\}$ which implies that there is no "power broadening" in these spectra.

One can note some interesting limiting forms of Eq. (4.2). If field α_1 is very strong ($\alpha_1>>|\Delta_{21}|$) such that $\theta\simeq\pi/4$, then Eq. (4.2) becomes

$$I(\Delta_{32})\simeq\frac{1}{4}\left[\frac{\Lambda_3}{\Gamma_3}-\frac{\Lambda_2+\Lambda_1}{\Gamma_2+\Gamma_1}\right]\left[\frac{\Gamma_3+\gamma_{21}}{\frac{1}{4}(\Gamma_3+\gamma_{21})^2+(\Delta_{32}+\frac{1}{2}\Delta_{21}-\alpha_1)^2}+\frac{\Gamma_3+\gamma_{21}}{\frac{1}{4}(\Gamma_3+\gamma_{21})^2+(\Delta_{32}+\frac{1}{2}\Delta_{21}+\alpha_1)^2}\right], \tag{4.5}$$

which reveals two resonances of the *same* amplitude and *same* width, centered at $\Delta_{32}=\pm\alpha_1-\frac{1}{2}\Delta_{21}$.

On the other hand, if $\Gamma_i<<\alpha_1<<|\Delta_{21}|$, then $\theta<<1$ and the $C-B$ resonance takes the form

$$\begin{aligned}I(\Delta_{32})_{CB}&\simeq\gamma_{32}(n_3^0-n_2^0)\left[\gamma_{32}^2+\left[\Delta_{32}-\frac{\alpha_1^2}{\Delta_{21}}\right]^2\right]^{-1}\\&\simeq\frac{\gamma_{32}(n_3^0-n_2^0)}{\gamma_{32}^2+\Delta_{32}^2}\left[1+\frac{2\alpha_1^2\Delta_{32}}{\Delta_{21}(\gamma_{32}^2+\Delta_{32}^2)}\right],\end{aligned} \tag{4.6}$$

which is a Lorentzian with a small *AC* Stark shift. If only the nonlinear part proportinal to α_1^2 is monitored, the *C*-*B* resonance has a dispersionlike shape.[33]

V. INHOMOGENEOUS BROADENING

According to (3.2) the probe response is negligible except near the resonances $\omega_{CB}=0$ and $\omega_{CA}=0$. The frequencies ω_{CB} and ω_{CA} are functions of $\tilde{\Delta}_{21}$, $\tilde{\Delta}_{32}$, and α_1. Since $\tilde{\Delta}_{21}$ and $\tilde{\Delta}_{32}$ depend on the atomic velocity which is determined by a distribution function and since, in principle, the value of α_1 might also be determined by a distribution function, the general resonance conditions can be satisfied by one or several atomic subgroups in the system. In this inhomogeneous broadening case, the atoms able to satisfy the resonance condition are those responsible for the probe response.

Many features of the probe spectra can be predicted with the aid of the simple graphical analysis given in Fig. 3. To use Fig. 3, it is useful to recall that $\omega_{CB}=\omega_C-\omega_B$ and $\omega_{CA}=\omega_C-\omega_A$, where ω_α is the energy of dressed state $|\alpha\rangle$ in units of $\hbar$ given by the diagonal elements of the Hamiltonian (2.14). In Fig. 3, ω_B and ω_A are plotted as a function of $\tilde{\Delta}_{21}$. A distribution of $\tilde{\Delta}_{21}$ is indicated schematically by the vertical-hatched column; the intersection of this hatched column with the ω_A and ω_B curves indicates the range of allowed values for ω_A and ω_B for this specific dis-

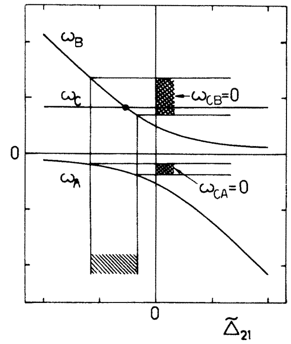

FIG. 3. Dressed-state frequencies ω_A, ω_B, and ω_C as a function of detuning $\tilde{\Delta}_{21}$. (The scales are in arbitrary frequency units.) The vertical strip gives the allowed values of $\tilde{\Delta}_{21}$ for some inhomogeneous distribution. As the probe is tuned, the ω_C line moves vertically and its intersection with the ω_A and ω_B curves gives the regions of probe absorption. These regions are indicated by the horizontal strips in the figure.

tribution of $\tilde{\Delta}_{21}$. The probe frequency (assumed to be independent of $\tilde{\Delta}_{21}$) appears as a horizontal line on this graph which moves vertically as the probe frequency is varied. The intersection of $\omega_C=\tilde{\Delta}_{32}$ with the allowed values of ω_A (or ω_B) gives the range over which the resonance conditions may be satisfied. These regions are indicated by the cross-hatched zones of Fig. 3.

The above analysis is modified somewhat if the variation in $\tilde{\Delta}_{21}$ is due to the Doppler effect.[34] In this case, a distribution of (axial) velocities

$$W(v)=\exp(-v^2/u^2)/\pi^{1/2}u\ , \tag{5.1}$$

where u is the most probable speed, leads to frequencies

$$\omega_A=-\tfrac{1}{2}(\Delta_{21}+k_1v)\\ -\tfrac{1}{2}[(\Delta_{21}+k_1v)^2+4\alpha_1^2]^{1/2}\ , \tag{5.2a}$$

$$\omega_B=-\tfrac{1}{2}(\Delta_{21}+k_1v)\\ +\tfrac{1}{2}[(\Delta_{21}+k_1v)^2+4\alpha_1^2]^{1/2}\ , \tag{5.2b}$$

$$\omega_C=\Delta_{32}+k_2v\ . \tag{5.2c}$$

For the sake of definiteness, we take $k_1>0$ and k_2 of arbitrary sign [see Eq. (2.4)] which simply corresponds to a choice of the direction of the positive z direction.

Inhomogeneously broadened three-level systems have been previously analyzed using a graphical approach.[15,17,22] We recall some well-known results and then discuss features not emphasized in earlier works.

To construct a graph similar to that in Fig. 3, we first define the dimensionless parameters

$$x=(\Delta_{21}+k_1v)/\alpha_1\ , \tag{5.3}$$

$$\omega'_\beta=\omega_\beta/\alpha_1\ \ (\beta=A,B,C)\ . \tag{5.4}$$

In terms of these parameters the quantity

$$\omega'_C=\nu+\frac{k_2}{k_1}x\ , \tag{5.5}$$

with

$$\nu=[\Delta_{32}-(k_2/k_1)\Delta_{21}]/\alpha_1 \tag{5.6}$$

is a linear function of x with slope of k_2/k_1 and y intercept of ν. In Fig. 4, the dimensionless frequencies $\omega'_A,\omega'_B,\omega'_C$ are plotted versus x. For a given Δ_{21} there is a range of x centered about $x=\Delta_{21}/\alpha_1$ of width $2k_1u/\alpha_1$ which determines the values of ω'_A and ω'_B present in the system. This range, which simply represents the inhomogeneous broadening in the system owing to the Doppler effect, is indicated by the vertical lines in Fig. 4. The intersection of ω'_C with ω'_A and ω'_B in this region determines possible resonances of the system since it corresponds to $\omega_{CB}=0$ or $\omega_{CA}=0$. As Δ_{32} is tuned, the ω'_C curve moves vertically and scans all possible resonances. The factors $\cos^2\theta$, $\sin^2\theta$, n_C^0, n_B^0, and n_A^0 which appear as weight factors for the resonances [see Eq. (3.2)] may be obtained from Fig. 5.

The velocity averaging is easily performed by noticing that for $\gamma_{\alpha\beta}<<|\omega_{\alpha\beta}|$ one can write

$$\frac{1}{\gamma_{CB}+i\omega_{CB}}\simeq-i\mathcal{P}\left[\frac{1}{\omega_{CB}}\right]\\ +\frac{\pi}{|\partial\omega_{CB}/\partial v|_{v=v_{CB}}}\delta(v-v_{CB})\ , \tag{5.7}$$

where $\omega_{CB}(v_{CB})=0$ and $|\partial\omega_{CB}/\partial v|_{v=v_{CB}}\neq0$ (v_{CB} is a simple zero of ω_{CB}). In the case $k_2/k_1>0$ (depicted in Fig. 4) the probe absorption is simply

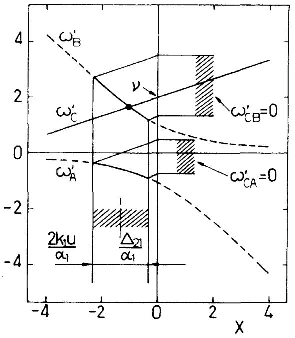

FIG. 4. A curve similar to Fig. 3 in which the dressed-state frequencies ω'_A, ω'_B, ω'_C (in units of α_1) are plotted as a function of velocity through the parameter $x=(\Delta_{21}+k_1v)/\alpha_1$. Since ω'_C varies linearly with v and, consequently, also linearly with x; the curve $\omega'_C(x)$ is a straight line of slope k_2/k_1 and ω' intercept $\nu=[\Delta_{32}-(k_2/k)\Delta_{21}]/\alpha_1$. The range of allowed x, indicated by the heavy portions of the ω'_A and ω'_B curves, is centered at Δ_{21}/α_1 and has a width determined by the Doppler distribution, which, in this case, is the inhomogeneous broadening mechanism. Tuning the probe corresponds to a vertical displacement of the ω'_C curve.

$$I(\Delta_{32})=\frac{\pi}{k_1}\left[W\left[\frac{\alpha_1 x-\Delta_{21}}{k_1}\right]\frac{\cos^2\theta(n_C^0-n_B^0)}{|\partial\omega'_{CB}/\partial x|}\bigg|_{x=x_{CB}}+W\left[\frac{\alpha_1 x-\Delta_{21}}{k_1}\right]\frac{\sin^2\theta(n_C^0-n_A^0)}{|\partial\omega'_{CA}/\partial x|}\bigg|_{x=x_{CA}}\right], \tag{5.8}$$

where the dimensionless velocity parameter x, Eq. (5.3), has been introduced.

Equation (5.8) together with Figs. 4 and 5 can be used to obtain some qualitative features of the probe spectrum. One first determines the allowed range of x contributing to the spectrum. Using Eq. (5.3) and the fact that $|v|\lesssim u$ it is seen that x must fall within the range defined by

$$\left| x-\frac{\Delta_{21}}{\alpha_1}\right| \lesssim \frac{k_1 u}{\alpha_1} . \tag{5.9}$$

This range of x, centered at Δ_{21}/α_1 with width of order $2k_1u/\alpha_1$, is indicated schematically by the heavy portions of ω'_A and ω'_B curves in Fig. 4. Having found the allowed range of x, one then proceeds as follows:

(1) The line $\omega'_C(x)$ [Eq. (5.5)] is drawn for each value of Δ_{32} (or, equivalently v) to determine the position, if any, of resonances $x=x_{CA}(v)$ or $x=x_{CB}(v)$ for which $\omega'_C=\omega'_A$ or $\omega'_C=\omega'_B$, respectively. Notice that a variation of v, which corresponds to varying the probe frequency, is represented in Fig. 4 by a vertical translation of the ω'_C line.

(2) At any resonance positions $x_{CA}(v)$, $x_{CB}(v)$, the corresponding weight functions $\cos^2\theta$, $\sin^2\theta$, $n_C^0-n_B^0$ and $n_C^0-n_A^0$ are read off of Fig. 5, and the velocity distribution $W[(\alpha_1 x-\Delta_{21})/k_1]$ is evaluated at $x=x_{CA}$ or $x=x_{CB}$.

(3) The final factor contributing in Eq. (5.8),

$$\frac{\partial\omega'_{C\alpha}}{\partial x}\bigg|_{x=x_{C\alpha}(v)}=\frac{\partial(\omega'_C-\omega'_\alpha)}{\partial x}\bigg|_{x=x_{C\alpha}(v)} \quad (\alpha=A,B) ,$$

is the *difference in slopes* between the ω'_C and ω'_α curves at the resonance positions. Using the above steps, one can construct the probe spectrum for various values of the parameters α_1, k_2/k_1 and Δ_{21}.

For positive slope $[k_2/k_1>0]$ of $\omega'_C(x)$, it is obvious from Fig. 4 that there always exists some values of v (i.e., probe detunings Δ_{32}) leading to *CA* and *CB* resonances. For k_2 negative (recall that we have arbitrarily taken $k_1>0$), both resonances still occur if $k_2(k_1+k_2)>0$ (magnitude of the slope of ω'_C greater than the magnitude of the slopes of the asymptotes of the ω'_B and ω'_A curves). On the other hand, if $k_2(k_1+k_2)<0$, ω_{CB} resonances are possible only if $v>0$ and ω_{CA} resonances only if $v<0$. There is a range of v

$$v^2\le v_{\rm cr}^2=4|k_2(k_1+k_2)|/k_1^2 \tag{5.10}$$

for which no resonances are possible and no probe absorption occurs.

Figures 6–9 illustrate the various cases. In Fig. 6 we have graphed $\omega'_{CA}(x,v)=0$ and $\omega'_{CB}(x,v)=0$ for the case $k_2>0$. As discussed above, for each value of x, there is one value of v for which $\omega_{CA}=0$ and one for which $\omega_{CB}=0$. By mapping out a horizontal strip giving the range of allowed x and projecting the intersection of this strip with the $\omega'_{CA}=0$ and $\omega'_{CB}=0$ curves onto the v axis, one obtains the range of $v=[\Delta_{32}-(k_2/k_1)\Delta_{21}]/\alpha_1$ for which significant probe absorption occurs.

If $k_1u>>\alpha_1$ and $|\Delta_{21}|\lesssim k_1u$, then x is centered at Δ_{21}/α_1 and the strip of allowed x has a large width $2k_1u/\alpha_1>>1$ which always includes $x=0$. In this case there is a wide range of v for which resonances occur as shown in Fig. 7(a). The *CA* and *CB* resonances overlap, leading to the typical probe spectrum shown in Fig. 7(a). For this case, the probe spectrum is given by (see Appendix C)

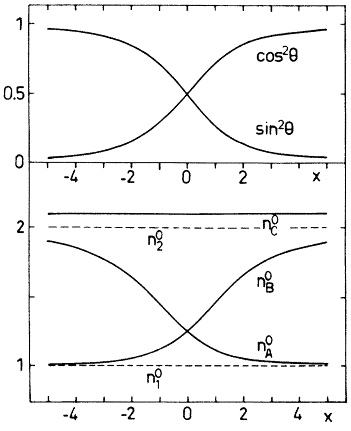

FIG. 5. Curves which give the weight factors $\sin^2\theta$, $\cos^2\theta$, n_α^0 $(\alpha=A,B,C)$ as a function of x. In the example shown, we have taken $n_1^0{:}n_2^0{:}n_3^0=1{:}2{:}2.1$ and $\Gamma_1{:}\Gamma_2=3{:}1$.

$$I(\Delta_{32})\simeq\frac{\pi^{1/2}}{|k_2|u}\exp\left[-\left[\frac{\Delta_{32}}{k_2}+\frac{\Delta_{32}+\Delta_{21}}{k_1+k_2}\right]^2\Big/4u^2\right]$$
$$\times\left[(n_3^0-n_2^0)+\frac{|k_2|}{\Gamma_2 k_1}(n_2^0-n_1^0)\frac{\alpha_1^2\gamma_{\text{eff}}}{[\Delta_{32}-(k_2/k_1)\Delta_{21}]^2+\gamma_{\text{eff}}^2\alpha_1^2/\Gamma_1\Gamma_2}\right], \tag{5.11}$$

where

$$\gamma_{\text{eff}}=\Gamma_1\frac{|k_2|}{k_1}+\Gamma_2\frac{|k_1+k_2|}{k_1}\ . \tag{5.12}$$

It consists of a broad background term representing linear absorption plus a strongly power-broadened Lorentzian of width $\alpha_1(\gamma_{\text{eff}}^2/\Gamma_1\Gamma_2)^{1/2}$. Although the ω_{CB} and ω_{CA} terms are not themselves Lorentzian, their sum is. Equation (5.11) may be obtained from Eq. (24) of Ref. 13 in the limit of large α_1^2.

For large detunings, $|\Delta_{21}|>>\alpha_1,k_1u$, the situation is depicted in Fig. 7b. The ω_{CB} and ω_{CA} resonances are now nonoverlapping, leading to the spectrum shown. In this limit

$$\omega_{CB}\simeq\Delta_{32}-\frac{\alpha_1^2}{\Delta_{21}}+k_2v\ , \tag{5.13a}$$

$$\omega_{CA}\simeq\Delta_{32}+\Delta_{21}+\frac{\alpha_1^2}{\Delta_{21}}+(k_1+k_2)v\ , \tag{5.13b}$$

and $\cos^2\theta\approx1$, $\gamma_{CB}\approx\gamma_{32}$, $\gamma_{CA}\approx\gamma_{31}$. The resulting spectrum is the sum of two Voigt profiles

$$I(\Delta_{32})\simeq\frac{n_3^0-n_2^0}{|k_2|u}Z_i\left[\frac{\Delta_{32}-\alpha_1^2/\Delta_{21}+i\gamma_{32}}{|k_2|u}\right]+\frac{\alpha_1^2}{\Delta_{21}^2}\frac{n_3^0-n_1^0}{|k_1+k_2|u}Z_i\left[\frac{\Delta_{32}+\Delta_{21}+\alpha_1^2/\Delta_{21}+i\gamma_{31}}{|k_1+k_2|u}\right], \tag{5.14}$$

where Z_i is the imaginary part of the plasma-dispersion function.[35] The spectral components are Gaussians if the arguments of Z_i have magnitude much less than unity and Lorentzians in the opposite limit.

For large intensities, $|\alpha_1|>>|\Delta_{21}|,k_1u$, the situation is depicted in Fig. 7c. In this limit both the central value and the range of x is much less than unity; the resulting spectrum arises from nonoverlapping *CA* and *CB* resonances. For this case we have

$$\omega_{CB}\simeq\Delta_{32}+\tfrac{1}{2}\Delta_{21}-\alpha_1+\left[k_2+\tfrac{1}{2}k_1-\frac{\Delta_{21}}{4\alpha_1}k_1\right]v-\frac{\Delta_{21}^2+k_1^2v^2}{8\alpha_1}\ , \tag{5.15a}$$

$$\omega_{CA}\simeq\Delta_{32}+\tfrac{1}{2}\Delta_{21}+\alpha_1+\left[k_2+\tfrac{1}{2}k_1+\frac{\Delta_{21}}{4\alpha_1}k_1\right]v+\frac{\Delta_{21}^2+k_1^2v^2}{8\alpha_1}\ , \tag{5.15b}$$

$\sin^2\theta\approx\cos^2\theta\approx\frac{1}{2}$, and $\gamma_{CB}\approx\gamma_{CA}\approx\frac{1}{2}(\gamma_{31}+\gamma_{32})$. Two (nearly) symmetric resonances appear at $\Delta_{32}=-\frac{1}{2}\Delta_{21}\pm\alpha_1$ and the spectrum is the sum of two Voigt profiles

$$I(\Delta_{32})\simeq\frac{1}{2}\left[\frac{\Lambda_3}{\Gamma_3}-\frac{\Lambda_2+\Lambda_1}{\Gamma_2+\Gamma_1}\right]\frac{1}{|k_2+\frac{1}{2}k_1|u}\left[Z_i\left[\frac{\Delta_{32}+\frac{1}{2}\Delta_{21}-\alpha_1+i\gamma_{CB}}{|k_2+\frac{1}{2}k_1|u}\right]+Z_i\left[\frac{\Delta_{32}+\frac{1}{2}\Delta_{21}+\alpha_1+i\gamma_{CA}}{|k_2+\frac{1}{2}k_1|u}\right]\right], \tag{5.16}$$

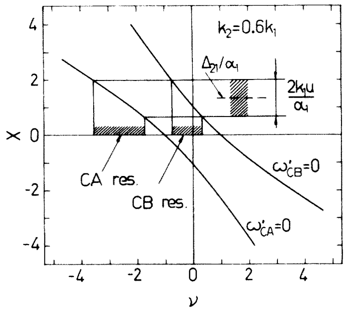

FIG. 6. Curves representing the resonance conditions $\omega'_{CA}(x,\nu)=0$ and $\omega'_{CB}(x,\nu)=0$ for the case $k_2>0$. For a range of allowed x determined by the detuning (Δ_{21}/α_1) and Doppler width (k_1u/α_1), one can find the regions of probe detuning (ν) for which absorption can occur. Conversely, for any value of probe detuning ν, one can determine whether or not any resonant velocity subset (x) can contribute to the signal. When $k_2>0$, there exists, for each value of ν, values of x for which both $\omega'_{CA}=0$ and $\omega'_{CB}=0$.

which are approximately Gaussians if the magnitude of the arguments of the Z_i functions are much less than unity. [In arriving at Eq. (5.16), we neglected the small $(\Delta_{21}^2+k_1^2v^2)/8\alpha_1$ terms in Eq. (5.15).]

The analysis is virtually unchanged if $k_2<0$ and $k_2(k_1+k_2)>0$. The ω'_A, ω'_B curves of Fig. 6 are rotated by 90° about the origin, but the same type of resonance conditions occur. If $k_1u>>\alpha_1$ and $|\Delta_{21}|\lesssim k_1u$, Eqs. (5.11) and (5.12) are still valid; γ_{eff} is now smaller than in the copropagating case owing to some Doppler-phase cancellation. Equations (5.14) and (5.16) remain valid for the large detuning and intense field limits. It is now possible, however, to have a narrow resonance in the large detuning case, provided that $k_2\simeq -k_1$.[36]

The remaining case $k_2(k_1+k_2)<0$ is represented in Fig. 8. As discussed above, there is a range of detunings ν $(\nu^2<\nu_{\text{cr}}^2)$ for which no resonance values of x may be found. For $\nu>\nu_{\text{cr}}$ two values of x correspond to the ω_{CB} resonance and, for $\nu<-\nu_{\text{cr}}$, two values of x correspond to the ω_{CA} resonance. The spectrum for the case $k_1u>>\alpha_1$, $|\Delta_{21}|\lesssim k_1u$ is shown in Fig. 9(a). For any $|\nu|>\nu_{\text{cr}}$, there are two velocity subgroups of atoms which contribute independently to the probe spectrum except in a region of width $\approx\Gamma$ near $|\nu|=\nu_{\text{cr}}$ where both contributions overlap. It is just this overlap region which gives rise to the non-power broadened resonances shown in Fig. 9(a). As derived in Appendix C, the spectrum for this case $(|\nu|\gtrsim\nu_{\text{cr}})$ is

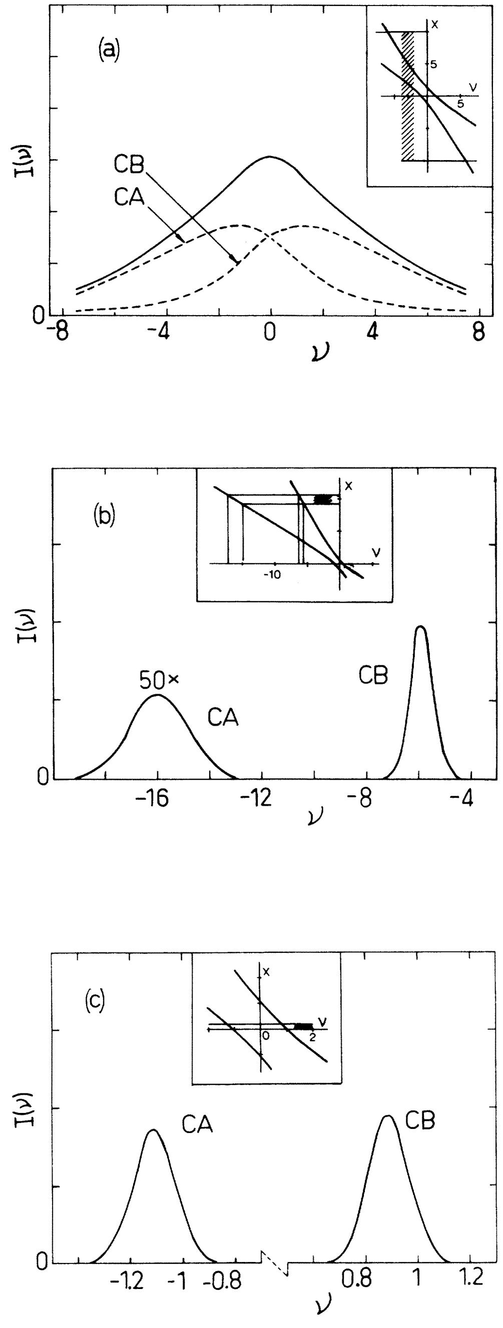

FIG. 7. Typical probe-absorption spectra (in arbitrary units) for the case $k_2=0.6k_1>0$ in the three limits (a) $k_1u>>\alpha_1$, $k_1u>|\Delta_{21}|$, (b) $|\Delta_{21}|>>\alpha_1$, k_1u, and (c) $\alpha_1>>k_1u$, $|\Delta_{21}|$. In drawing these curves, we have taken $n_1^0:n_2^0:n_3^0=1:3:4$ and $\Gamma_1=\Gamma_2<<\alpha_1$. In (a), $\Delta_{21}=0$ and $k_1u=10\alpha_1$; in (b), $\Delta_{21}=10\alpha_1$ and $k_1u=\alpha_1$; in (c), $\Delta_{21}=k_1u=0.1\alpha_1$. The inserts are curves analogous to Fig. 6 and indicate the resonant-velocity subgroups which contribute to the probe absorption at a given value of ν.

$$I(\nu)=\frac{1}{k_1u}\left[\frac{2\pi(k_1+k_2)}{|k_2|}\right]^{1/2}\exp\left[-\left[\Delta_{21}-\alpha_1\frac{(k_1+2k_2)}{[\,|k_2|(k_1+k_2)]^{1/2}}\right]^2\Big/k_1^2u^2\right]$$
$$\times\left[(n_3^0-n_2^0)+\frac{\Gamma_1|k_2|(n_2^0-n_1^0)}{\Gamma_1|k_2|+\Gamma_2|k_1+k_2|}\right]\mathrm{Re}\left\{\left[|\nu|-\nu_{\mathrm{cr}}-\frac{i}{\alpha_1}\left[\frac{|k_2|}{k_1}\gamma_{31}+\frac{k_1+k_2}{k_1}\gamma_{32}\right]\right]^{-1/2}\right\}. \tag{5.17}$$

The large detuning and large field intensity limits are depicted in Figs. 9(b) and 9(c), respectively. Equations (5.14) and (5.16) may still be used to describe these profiles. For the intense field case, a narrow resonance occurs if $k_2\simeq -k_1/2$.

The Doppler-free nature of the narrow resonances which may occur when $\alpha_1 >> k_1u$ or $|\Delta_{21}| >> k_1u, \alpha_1$ arises from a cancellation of Doppler phases. All atoms contribute equally to these resonances; this feature is easily seen in Fig. 4. If $\alpha_1 >> k_1u$, the range of allowed values of x narrows considerably and the heavy portions of the ω_A' and ω_B' curves reduce to points. If the ω_C' curve is tangent to the ω_A' or ω_B' curves at these points, then all atoms contribute to the resonance. This condition is

$$\frac{k_2}{k_1}=-\frac{1}{2}\pm\frac{1}{2}\frac{\Delta_{21}}{(\Delta_{21}^2+4\alpha_1^2)^{1/2}} \tag{5.18}$$

leading to narrow resonances centered at

$$\Delta_{32}=-\tfrac{1}{2}\Delta_{21}\pm\tfrac{1}{2}(\Delta_{21}^2+4\alpha_1^2)^{1/2}\,, \tag{5.19}$$

where the upper (lower) signs refer to the $\omega_C'=\omega_B'$ ($\omega_C'=\omega_A'$) resonance. If $|\Delta_{21}| >> k_1u, \alpha_1$, the allowed x values are located on the asymptotes of

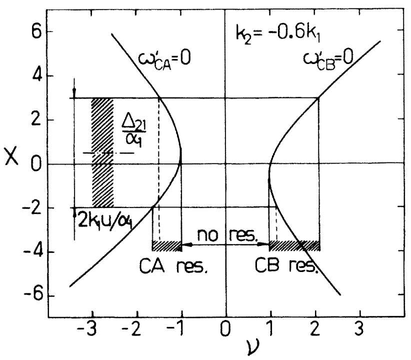

FIG. 8. Resonance conditions $\omega_{CA}'(x,\nu)=0$ and $\omega_{CB}'(x,\nu)=0$ for the case $-k_1<k_2<0$. There is now a range of $|\nu|<\nu_{\mathrm{cr}}$ for which there are no resonant-velocity groups of atoms.

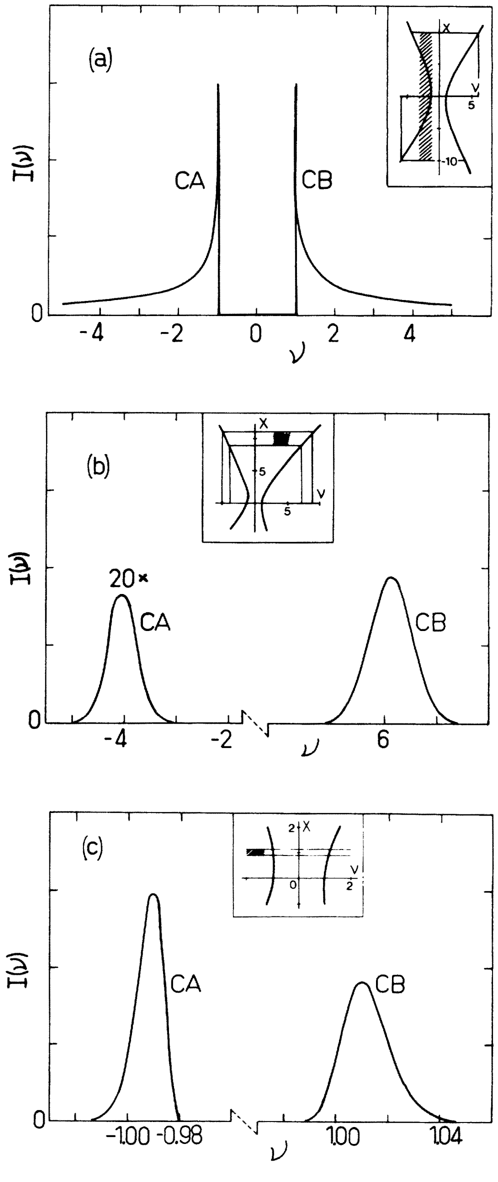

FIG. 9. Probe-absorption spectra for the case $k_2/k_1=-0.6$, but otherwise the same conditions as in Fig. 7. Note that, owing to Doppler-phase cancellation, the resonances are narrower than those in the corresponding spectra of Fig. 7.

the ω'_A and ω'_B curves. By having $k_2=-k_1$, the ω'_C curve coincides with these asymptotes so that all atoms once again contribute. Since the resonance condition is the same for all the atoms, the resulting resonance is narrow.

On the other hand, when $\alpha_1 << k_1 u, |\Delta_{21}| \lesssim k_1 u$ only a limited velocity subset of atoms, determined by the pump intensity and detuning (i.e., $|k_1 v+\Delta_{21}| \lesssim \alpha_1$), contribute to the probe absorption. The resulting linewidths are smaller than the Doppler width, reflecting the narrower range of contributing velocity groups.

VI. EXTENSIONS OF THE DAP APPROACH

The DAP allows one to gain physical insight into problems involving more complicated atom-field interactions. The dressed-energy levels of a multilevel atom can be solved exactly or approximately. The weight factors of the spectra which involve elements of the transformation matrix from the bare to dressed picture are generally more difficult to obtain. For dressed-energy-level separations much greater than the natural widths of the levels, a rate-type solution to the DAP equations may be used. In this section, some features of a four-level problem and a three-level problem involving a standing-wave pump field are discussed. In Sec. VII some aspects of coherent transients are examined using the DAP formalism.

A. Strongly coupled three-level system[12,15,19,37–41]

We first consider a three-level system in which one must now diagonalize the complete Hamiltonian. The eigenvalue equation

$$\omega(\omega+\tilde{\Delta}_{21})(\omega-\tilde{\Delta}_{32})-\alpha_2^2(\omega+\tilde{\Delta}_{21}) -\alpha_1^2(\omega-\tilde{\Delta}_{32})=0 \tag{6.1}$$

always has three real roots ω_α ($\alpha=A,B,C$). Equations (2.23) now take the form

$$\dot{\tilde{\rho}}_{\alpha\alpha}=\Lambda_\alpha-\Gamma_\alpha\tilde{\rho}_{\alpha\alpha}+\sum_{\sigma,\delta}R_{\alpha\alpha;\sigma\delta}\tilde{\rho}_{\sigma\delta} , \tag{6.2a}$$

$$\dot{\tilde{\rho}}_{\alpha\beta}=\Lambda_{\alpha\beta}-(\gamma_{\alpha\beta}+i\omega_{\alpha\beta})\tilde{\rho}_{\alpha\beta}+\sum_{\sigma,\delta}R_{\alpha\beta;\sigma\delta}\tilde{\rho}_{\sigma\delta} , \tag{6.2b}$$

where the coefficients are functions of the transformation matrix elements $\langle i | \alpha \rangle$. The coupling coefficients $R_{\alpha\beta,\sigma\delta}$ are all proportional to differences between decay rates Γ_i. The $\omega_{\alpha\beta}=\omega_\alpha-\omega_\beta$ are the frequency separations between the dressed states. If $|\omega_{\alpha\beta}| >> \Gamma_i$, the off-diagonal density-matrix elements are small and an approximate solution to Eqs. (6.2) is

$$\tilde{\rho}^0_{\alpha\alpha}=\Lambda_\alpha/\Gamma_\alpha=n^0_\alpha , \tag{6.3a}$$

$$\tilde{\rho}^0_{\alpha\beta}=-i\left[\Lambda_{\alpha\beta}+\sum_\sigma R_{\alpha\beta;\sigma\sigma}n^0_\sigma\right]\omega^{-1}_{\alpha\beta} . \tag{6.3b}$$

Transforming back to the coordinate system $|i\rangle$ we obtain the observables $\tilde{\rho}_{ii}$, $\tilde{\rho}_{21}$, or $\tilde{\rho}_{32}$. In the special case when all Γ's are equal ($\Gamma_i=\gamma$), the coupling coefficients $R_{\alpha\beta,\sigma\delta}$ vanish, and the exact solution is simply

$$\tilde{\rho}^0_{\alpha\alpha}=\Lambda_\alpha/\gamma , \tag{6.4a}$$

$$\tilde{\rho}^0_{\alpha\beta}=\Lambda_{\alpha\beta}/(\gamma+i\omega_{\alpha\beta}) . \tag{6.4b}$$

In this limit, the absorption spectrum for field α_2 is

$$I(\Delta_{32})=-\frac{1}{\alpha_2}\sum_{\alpha,\beta}\frac{\omega_{\alpha\beta}\langle 3|\alpha\rangle\langle\beta|2\rangle\Lambda_{\alpha\beta}}{\gamma^2+\omega^2_{\alpha\beta}} , \tag{6.5}$$

where $\Lambda_{\alpha\alpha}\equiv\Lambda_\alpha$ and $\omega_{\alpha\alpha}=0$. Once the transformation matrix elements are known this formula is useful for analyzing the strong-field absorption (cf. the corresponding rather lengthy expression of the BAP). The solution is more complicated when interlevel relaxation is allowed or the decay rates differ greatly. Then the spectrum must be obtained using Eq. (6.2) or (6.3) together with the transformation back to the BAP.

B. Four-level systems[42–44]

As shown previously, the DAP is especially transparent when one of the fields is weak and the strongly coupled part satisfies the rate-type solution. This result can be applied to a four-level system in which levels 1,2,3 are strongly coupled by fields α_1 and α_2 and one of these levels is weakly coupled by a probe field to level 4. The corresponding dressed states are labeled A,B,C,D where D is the weakly coupled state. To obtain the resonance positions we have to solve Eq. (6.1). A graphical solution is shown in Fig. 10 for fixed α_2 as a function of α_1. Whenever $\omega_D=\omega_\alpha$ ($\alpha=A,B,C$) a probe resonance results. A rate-type solution obviously requires that the anticrossing in Fig. 10 is

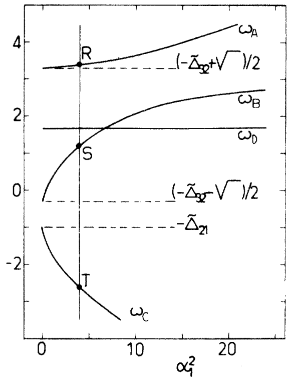

FIG. 10. Dressed-atom frequencies as a function of α_1^2 for $\alpha_2=1$, $\tilde{\Delta}_{21}=1$, and $\tilde{\Delta}_{32}=3$ (all frequencies are in arbitrary units and it is assumed that all relaxation parameters have values much less than one in these units). The horizontal broken lines give the dressed-atom frequencies when $\alpha_1=0$. For a fixed α_1, there are generally three possible probe resonances as the probe frequency $\omega_D=\tilde{\Delta}_D$ is varied. For $\alpha_1^2=4$, these positions are indicated by the points R, S, and T.

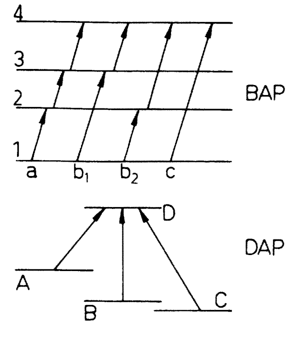

FIG. 11. A classification of the atom-field interactions for four-level systems in both the BAP and DAP. The BAP interpretation, valid only to lowest orders in the fields, is (a) stepwise absorption of α_1, α_2, α_3, (b_1) two-photon absorption of α_1 and α_2 followed by absorption of α_3, (b_2) absorption of α_1 followed by two-photon absorption of α_2 and α_3, and (c) three-photon absorption of α_1, α_2, and α_3. In the DAP, valid at any field intensities, there are three, single-photon processes which contribute to the absorption. For intense fields α_1 and α_2 the single-photon processes do not interfere.

large compared to relaxation rates.

If Doppler broadening is present one may ask whether a splitting similar to the one appearing in three-level systems with $k_2(k_1+k_2)<0$ also occurs in four-level systems. In three-level systems, the splitting shown in Fig. 9 is caused by the absence of resonant-velocity subgroups of atoms over a range of probe detunings. In a four-level system, a resonance occurs when $\omega_D \equiv \Delta_D + k_D v$ is equal to any of the solutions $\omega_\alpha(v)$ of Eq. (6.1). Using the Doppler-shifted values of all the detunings $\tilde{\Delta}_{ij}$ and substituting ω_D for ω in Eq. (6.1), one obtains a cubic equation for v which always has at least one real root.[45] This result implies that there is always at least one resonant-velocity subgroup for all probe detunings of the four-level system. Thus, the mechanism operative in three-level systems leading to the split spectrum of Fig. 9 cannot occur here. The details of the probe spectrum may depend on the number of resonant velocity subgroups contributing (i.e., one or three), but this feature has yet to be investigated. (Notice that in a five-level system, the quartic eigenvalue equation can have 0, 2, or 4 real roots. The absence of real roots signals a splitting effect similar to that shown in Fig. 9.)

A comparison between the BAP and DAP pictures for a four-level system is shown in Fig. 11 in which the probe acts between levels 3 and 4. The BAP nomenclature is valid in the small-intensity limit only. Note that the processes a and b_1 have the same resonance condition ($\tilde{\Delta}_{43}=0$) and provide two interfering channels for this resonance. The DAP consists of three noninterfering single-photon transitions allowing for a very simple physical interpretation.

In some special cases, Eq. (6.1) is easily solved, e.g.,

$$\text{(i)}\ \tilde{\Delta}_{21}=\tilde{\Delta}_{32}=0;\ \ \omega_{A,C}=\pm(\alpha_1^2+\alpha_2^2)^{1/2},\ \ \omega_B=0\ ;$$

$$\text{(ii)}\ \tilde{\Delta}_{21}=\tilde{\Delta}_{32},\alpha_1^2=\alpha_2^2;\ \ \omega_{A,C}=\pm(\tilde{\Delta}_{21}^2+2\alpha_1^2)^{1/2},\ \ \omega_B=0\ ;$$

$$\text{(iii)}\ \tilde{\Delta}_{21}=-\tilde{\Delta}_{32},\alpha_1^2=\alpha_2^2;\ \ \omega_{A,C}=-\tfrac{1}{2}\tilde{\Delta}_{21}\pm\tfrac{1}{2}(\tilde{\Delta}_{21}^2+8\alpha_1^2)^{1/2},\ \ \omega_B=-\tilde{\Delta}_{21}\ .$$

As an example let us consider the case (ii) in which $\alpha_1=\alpha_2=\alpha$. The transformation is now

$$|A\rangle=\frac{1}{2}\left[1-\frac{\tilde{\Delta}_{21}}{\Omega_R}\right]|1\rangle+\frac{\alpha}{\Omega_R}|2\rangle+\frac{1}{2}\left[1+\frac{\tilde{\Delta}_{21}}{\Omega_R}\right]|3\rangle\ , \tag{6.6a}$$

$$|B\rangle=(\alpha\,|1\rangle+\tilde{\Delta}_{21}\,|2\rangle-\alpha\,|3\rangle)/\Omega_R\ , \tag{6.6b}$$

$$|C\rangle=\frac{1}{2}\left[1+\frac{\tilde{\Delta}_{21}}{\Omega_R}\right]|1\rangle-\frac{\alpha}{\Omega_R}\,|2\rangle+\frac{1}{2}\left[1-\frac{\tilde{\Delta}_{21}}{\Omega_R}\right]|3\rangle\ , \tag{6.6c}$$

where $\Omega_R=(\Delta_{21}^2+2\alpha^2)^{1/2}$, $\omega_A=\Omega_R$, $\omega_B=0$, and $\omega_C=-\Omega_R$. If the probe couples levels 4 and 2 ($\omega_D=\tilde{\Delta}_{42}$), if all the γ's are equal and if only level 4 is initially populated the response is simply

$$I(\tilde{\Delta}_{42})=\frac{\gamma n_4^0}{\Omega_R^2}\left[\frac{\alpha^2}{\gamma^2+(\tilde{\Delta}_{42}-\Omega_R)^2}+\frac{\tilde{\Delta}_{21}^2}{\gamma^2+\tilde{\Delta}_{42}^2}+\frac{\alpha^2}{\gamma^2+(\tilde{\Delta}_{42}+\Omega_R)^2}\right]. \tag{6.7}$$

The absorption spectrum consists of three Lorentzians.[19]

Equation (6.7) is applicable to the level scheme in Fig. 12 ($k_1=-k_2=k_D=k$) for which

$$\tilde{\Delta}_{21}=\Delta_{21}+kv\ (\Delta_{21}=\omega_{21}-\Omega_1)\ ,\ \ \tilde{\Delta}_{32}=-\Delta_{21}+kv\ ,\ \ \tilde{\Delta}_{42}=-\Delta_{24}-kv\ (\Delta_{24}=\omega_{24}-\Omega_2)\ .$$

If $\Delta_{21}=0$, the conditions for (6.7) are satisfied ($\tilde{\Delta}_{32}=\tilde{\Delta}_{21}=kv$, $\alpha_1^2=\alpha_2^2=\alpha^2$) and we get

$$I(\Delta_{24})=\frac{n_4^0\gamma}{(k^2v^2+2\alpha^2)}\left[\frac{\alpha^2}{\gamma^2+[\Delta_{24}+kv+(k^2v^2+2\alpha^2)^{1/2}]^2}+\frac{k^2v^2}{\gamma^2+(\Delta_{24}+kv)^2}+\frac{\alpha^2}{\gamma^2+[\Delta_{24}+kv-(k^2v^2+2\alpha^2)^{1/2}]^2}\right]. \tag{6.8}$$

The velocity-averaged probe-absorption spectrum (assuming $ku>>\gamma$) is given by

$$I(\Delta_{24})\simeq\frac{n_4^0\pi^{1/2}}{ku}\exp\left[-\frac{\Delta_{24}^2}{k^2u^2}\right]. \tag{6.9}$$

There is no narrow structure in the spectrum. The result should be contrasted with the structure obtained when a standing-wave saturator is used (see Fig. 12 and the discussion below).

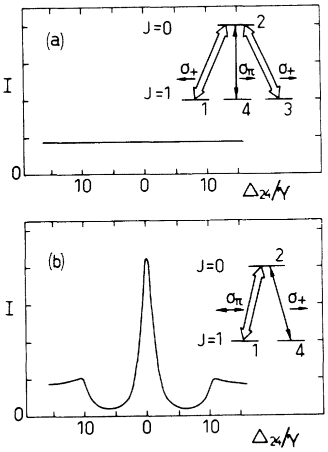

FIG. 12. (a) A four-level scheme in which levels 1,3,4 are degenerate levels of a $J=1$ state while level 2 is a $J=0$ state. The strong fields counterpropagate, are circularly polarized, and are resonantly tuned ($\Delta_{21}=0$). The probe field is π polarized and acts on the 2-4 transition. The probe absorption spectrum I for this case is flat. (b) For comparison, the probe-absorption spectrum for a three-level system with a standing-wave saturator is shown (see Ref. 53).

C. Standing-wave saturator (two-mode pump)[46–59]

As is well known, the interpretation of the spectra obtained with a standing-wave (SW) saturator is considerably more complicated than the running-wave case.[46–53] Similar difficulties are encountered when the saturator is composed of two running-wave fields having different frequencies.[54–59] The question arises as to whether or not the DAP offers any simplifications.

In the rotating-wave approximation the equation of motion of the density-matrix retains a periodic time dependence owing to the beat frequency $\delta=\Omega_2-\Omega_1$ between the two saturator modes; in the SW case, this beat frequency is twice the Doppler shift, $\delta=2k_1v$. According to the Floquet theorem,[54] the stationary solution to the system contains Fourier components with frequencies $\omega_{A,B}(n)=\omega_{A,B}+n\delta$ ($n=0,\pm1,\dots$), where ω_A and ω_B are functions of the mode amplitudes and detunings and are chosen such that $|\omega_{AB}|<|\delta|$. These frequencies are related to the eigenfrequencies of the DAP. The states $|1,n_1,n_2\rangle$ and $|2,m_1,m_2\rangle$ are nearly degenerate if

$$n_1+n_2=m_1+m_2+1=N\ ,$$

where n_i and m_i are the number of photons in mode i and we have assumed $\omega_{21}>0$. For a fixed total number of photons N there is an "infinite" ($\simeq 2\times N$) number of bare-atom states which must be diagonalized. The diagonalization, which can be performed using continued fractions, is not done here. Instead we concentrate on some qualitative aspects of the problem.

If the mode spacing δ is fixed, a rate-type solution in the DAP is valid provided that both $|\delta-\omega_{BA}|>>\gamma$ and $\omega_{AB}>>\gamma$ $(\omega_{BA}=\omega_B-\omega_A>0)$. Similarly to the running-wave case, probe resonances are found when $\omega_C=\omega_{A,B}+n\delta$, where ω- corresponds to the probe detuning (recall that the probe couples to a third, unperturbed level). The heights of the various peaks generally depend in a complicated way on the detunings and amplitudes of the saturator modes.

For a SW saturator the beat frequency $\delta=2k_1v$ is velocity dependent. Difficulties arise since, for slow enough atoms, the energy levels in the DAP form a quasicontinuum. Thus a rate-type solution for the DAP is clearly not applicable for $|2k_1v|\lesssim\gamma$. This region must be described by other approximations. For instance, in the limit $v\rightarrow 0$, the atoms are stationary and the probe response is readily calculated.[52]

Some qualitative understanding of the SW problem is obtained by constructing DAP energy-level diagrams similar to those of the running-wave case (see Fig. 4). Two examples are shown in Figs. 13 and 14.

In Fig. 13, we display the dressed-energy levels as a function of k_1v for a SW saturator with detuning $|\Delta_{21}|>\alpha$. The standing wave consists of two running-wave components labeled by $(\alpha_+,\ k_+=k_1>0)$ and $(\alpha_-,\ k_-=-k_1)$. In the region $k_1v<<-\gamma$ (assuming $\Delta_{21}>0$), we can, to a first approximation, use the unperturbed energy levels $\omega_{A,B}$ associated with the running wave α_+ since the wave α_- is strongly detuned and acts only as a perturbation in the region $k_1v<<-\gamma$. The dressed-level frequencies associated with the α_+ wave are given by [see Eq. (5.2)]

$$\omega_{A,B}(n)\approx-\tfrac{1}{2}(\Delta_{21}+k_1v)\mp\tfrac{1}{2}[(\Delta_{21}+k_1v)^2+4\alpha_+^2]^{1/2}+2nk_1v\ . \tag{6.10}$$

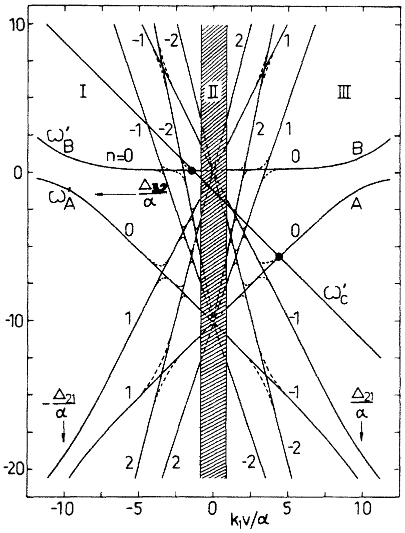

FIG. 13. Dressed-state frequencies $\omega'_A(n)=\omega'_A+2nk_1v/\alpha$, $\omega'_B(n)=\omega'_B+2nk_1v/\alpha$, and $\omega'_C=(\Delta_{32}+k_2v)/\alpha$ $(k_2\simeq-k_1)$ as a function of k_1v for a large-field detuning $|\Delta_{21}|>>\gamma$. Values for n are given by the integers labeling each curve. All frequencies are expressed in units of α; the detunings are $\Delta_{21}/\alpha=10$ and $\Delta_{32}/\alpha=-1$. In the range $\gamma<|k_1v|<|\Delta_{21}|$, the frequencies $\omega_A(n)$ and $\omega_B(n)$ are approximately given by $\omega_A(n)=-\Delta_{21}+|k_1v|+2nk_1v$ and $\omega_B(n)=2nk_1v$. The diagram may be used to determine resonance conditions in regions I and III, but not in region II where the rate-type solutions of the DAP break down. Resonant-velocity groups are determined by the intercept of the ω'_C curve with the curves $\omega'_{A,B}(n)$. In the example shown, the major contributions to the probe response arise from the crossings denoted by the large dots (see Fig. 4 of Ref. 53).

Equation (6.10) is not strictly applicable at any value of k_1v where two of the eigenfrequencies are degenerate. At such points, we must use degenerate perturbation theory: the net result is that the crossings are transformed into anticrossings owing to the action of the saturator mode α_-. The energy levels are sketched in Fig. 13.

In the region $k_1v>>\gamma$, the roles of α_+ and α_- are interchanged; the corresponding dressed-level frequencies are given by Eq. (6.10) with the replacement of k_1 by $-k_1$ and α_+ by α_-.

In the intermediate region $-\gamma<k_1v<\gamma$, the rate-type solution of DAP fails. There one may, as a first approximation, use the results valid for $v=0$ discussed in Sec. IV modified to incorporate the standing-wave nature of the saturator. In this region Eq. (6.10) is replaced by

$$\omega_{A,B}\simeq-\tfrac{1}{2}\Delta_{21}\mp\tfrac{1}{2}[\Delta_{21}^2+4\alpha(z)^2]^{1/2}\ , \tag{6.11}$$

where

$$\alpha(z) = |\alpha_+ e^{-ik_1 z} + \alpha_- e^{ik_1 z}| \ . \tag{6.12}$$

The inhomogeneity in $\omega_{A,B}$, owing to the z dependence of $\alpha(z)$, can be treated by the methods outlined at the beginning of Sec. V.

Tuning the probe corresponds to moving the line $\omega_C = \Delta_{32} + k_2 v$ vertically. For each value of Δ_{32} there exists an infinite number of resonant subgroups v satisfying the condition $\omega_C(v) = \omega_{A,B}(v,n)$. Whether these resonance subgroups really manifest themselves in the probe absorption depends on the magnitude of the various weight factors derived from the BAP→DAP transformation. For example, in the case shown in Fig. 13, the two major resonant-velocity subgroups are determined at the intersection parts of the ω_C' and dressed states shown in the figure. For other detunings, one can map out the contributing resonant-velocity subgroups and obtain qualitative agreement with the numerically calculated curves of Fig. 4 of Ref. 53.

Figure 14 represents the case of a resonantly tuned SW saturator ($\alpha_+ = \alpha_- = \alpha$) for which the exact DAP energy levels are given by[46–59]

$$\omega_{A,B}(n) = nk_1 v$$

$$\omega_A(n) = -|k_1 v| + 2nk_1 v \ , \quad \omega_B(n) = 2nk_1 v \ .$$

The method for determining possible resonant-velocity subgroups remains the same. It should be stressed that this method indicates the positions of possible resonant structure. The determination of the weights associated with these resonances represents a much more complicated problem.[46–59] The striking difference in probe response for running- and standing-wave saturators is illustrated in Fig. 12. The structure observed in Fig. 12(b) has its origin in the various harmonics which enter when a standing-wave saturator is used (but are absent for traveling-wave saturators).

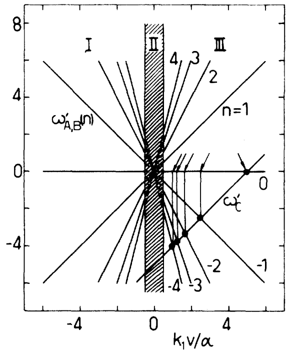

FIG. 14. A diagram corresponding to Fig. 13 for a resonantly tuned ($\Delta_{21}=0$), standing-wave saturator. In this case, the exact dressed-level frequencies are given by $\omega'_{A,B}(n) = nk_1 v/\alpha$ [$\omega_A(n) = -|k_1 v| + 2nk_1 v$; $\omega_B(n) = 2nk_1 v$]. We have chosen a probe with detuning $\Delta_{32}/\alpha = -5$ and propagation vector $\vec{k}_2 \simeq \vec{k}_1$ such that $\omega'_C \simeq -5 + k_1 v/\alpha$. Some of the resonant-velocity groups indicated by the arrows manifest themselves as distinct peaks in the velocity-dependent probe response (see Fig. 2 of Ref. 53).

VII. DAP TRANSIENTS

A. Two-level system

The steady-state spectra have been given a simple physical interpretation using the DAP. It is interesting to study also transient behavior using the DAP.[60] For simplicity we assume that $\Gamma_2 = \Gamma_1 = \gamma$ in which case the DAP equation of motion for the AB system is simply

$$\dot{\tilde{\rho}}_{AA} = \Lambda_A - \gamma \tilde{\rho}_{AA} \ , \tag{7.1a}$$

$$\dot{\tilde{\rho}}_{BB} = \Lambda_B - \gamma \tilde{\rho}_{BB} \ , \tag{7.1b}$$

$$\dot{\tilde{\rho}}_{BA} = \Lambda_{BA} - (\gamma + i\omega_{BA}) \tilde{\rho}_{BA} \ . \tag{7.1c}$$

[Notice that we have assumed $\alpha_1 =$constant; therefore, Eq. (7.1) can be applied only for stepwise changes of α_1.]

Assume that field α_1 is switched on at time $t=0$ leading to an optical nutation signal in the BAP. The solution of the DAP equations (7.1) is

$$\tilde{\rho}_{aa}(t) = (\Lambda_a/\gamma)(1 - e^{-\gamma t}) + \tilde{\rho}_{aa}(0) e^{-\gamma t} \ , \tag{7.2a}$$

$$\tilde{\rho}_{BA}(t)=\left[\frac{\Lambda_{BA}}{\gamma+i\omega_{BA}}\right](1-e^{-(\gamma+i\omega_{BA})t})+\tilde{\rho}_{BA}(0)e^{-(\gamma+i\omega_{BA})t}\ . \tag{7.2b}$$

The populations show a simple exponential decay towards their new equilibrium. The oscillatory nutation-type behavior is contained in $\tilde{\rho}_{BA}$. The initial conditions, obtained from (2.29) for an incoherent initial state, are given by

$$\tilde{\rho}_{AA}(0)=n_1^0\cos^2\theta+n_2^0\sin^2\theta\ , \tag{7.3a}$$

$$\tilde{\rho}_{BB}(0)=n_1^0\sin^2\theta+n_2^0\cos^2\theta\ , \tag{7.3b}$$

$$\tilde{\rho}_{BA}(0)=\tfrac{1}{2}(n_1^0-n_2^0)\sin 2\theta\ . \tag{7.3c}$$

Using Eqs. (2.24) and (7.3) in Eqs. (7.2), we find

$$\tilde{\rho}_{\alpha\alpha}(t)=\tilde{\rho}_{\alpha\alpha}(0)\ , \tag{7.4a}$$

$$\tilde{\rho}_{BA}(t)=\tfrac{1}{2}(n_1^0-n_2^0)\sin 2\theta\left[\frac{\gamma}{\gamma+i\omega_{BA}}(1-e^{-(\gamma+i\omega_{BA})t})+e^{-(\gamma+i\omega_{BA})t}\right]. \tag{7.4b}$$

The dressed-atom populations remain constant during the transient. If $\omega_{BA}>>\gamma$ we can write

$$\tilde{\rho}_{BA}(t)=\tilde{\rho}_{BA}(0)e^{-(\gamma+i\omega_{BA})t}\ . \tag{7.5}$$

Nutation in the BAP corresponds to free-induction decay in the DAP. In the BAP the switching on of α_1 creates the coherence $\tilde{\rho}_{21}$, while, in the DAP, the same change destroys the initial coherence $\tilde{\rho}_{BA}(0)$. According to (2.29) all the observables $\tilde{\rho}_{11}$, $\tilde{\rho}_{22}$, and $\tilde{\rho}_{21}$ depend on $\tilde{\rho}_{BA}$ and, therefore, reflect the decay of $\tilde{\rho}_{BA}$.

The DAP does not offer any substantial advantages over the BAP in calculating the free-induction decay or photon echo of a two-level system (although it may be useful for nutation echoes).[61] In both cases, the field is off for a long time period between the pulses when the BAP and DAP coincide. The DAP is a more natural approach when a strong-field—atomic-interaction occurs.

B. Three-level transients[62–72]

The DAP can provide a useful description of three-level transients. For a strong pump field α_1 and a weak probe α_2, Eqs. (2.23) give the time evolution of the system in the dressed basis. The DAP is most useful if either (1) field α_1 is constant and field $\alpha_2(t)$ undergoes some transient behavior leading to optical nutation, free-induction decay, photon echo, etc. on the *BC* and *AC* transitions (see Fig. 1) or (2) the field α_1 is switched on at some time and α_2 may have an arbitrary time dependence.

We consider first the case when α_1 is constant and α_2 is switched on at $t=0$. Equations (2.23) and (2.29) describing the probe response are (assuming $\Gamma_1=\Gamma_2=\gamma$)

$$\dot{\tilde{\rho}}_{CA}=-(\gamma_{CA}+i\omega_{CA})\tilde{\rho}_{CA}-i\alpha_2\sin\theta(\tilde{\rho}^0_{CC}-\tilde{\rho}^0_{AA})-i\alpha_2\cos\theta\tilde{\rho}^0_{BA}\ , \tag{7.6a}$$

$$\dot{\tilde{\rho}}_{CB}=-(\gamma_{CB}+i\omega_{CB})\tilde{\rho}_{CB}+i\alpha_2\cos\theta(\tilde{\rho}^0_{CC}-\tilde{\rho}^0_{BB})+i\alpha_2\sin\theta\tilde{\rho}^0_{AB}\ , \tag{7.6b}$$

$$\tilde{\rho}_{32}=\cos\theta\tilde{\rho}_{CB}-\sin\theta\tilde{\rho}_{CA}\ , \tag{7.7}$$

subject to the initial conditions $\tilde{\rho}_{CA}(0)=\tilde{\rho}_{CB}(0)=0$.

The $\tilde{\rho}^0_{\alpha\beta}$ are the *steady-state* dressed-atom density-matrix elements. Solving Eqs. (7.6) using the steady-state values $\tilde{\rho}^0_{\alpha\alpha}=\Lambda_\alpha/\gamma=n^0_\alpha$, $\tilde{\rho}^0_{AB}\simeq 0$, and $\tilde{\rho}^0_{BA}\simeq 0$, we obtain

$$\tilde{\rho}_{32}(t)=\frac{i\alpha_2\sin^2\theta(n_C^0-n_A^0)}{\gamma_{CA}+i\omega_{CA}}(1-e^{-(\gamma_{CA}+i\omega_{CA})t})+\frac{i\alpha_2\cos^2\theta(n_C^0-n_B^0)}{\gamma_{CB}+i\omega_{CB}}(1-e^{-(\gamma_{CB}+i\omega_{CB})t})\ . \tag{7.8}$$

The oscillatory behavior which appears in homogeneously broadened systems may disappear if inhomogeneous broadening is present. The oscillations may, however, remain observable if ω_{CA} or ω_{CB} depend only weakly on the atomic velocity. As an example let us consider the case when (5.15) is valid. The velocity-averaged CA contribution is (taking $n_1^0=n_2^0=0$)

$$\langle\widetilde{\rho}_{32}(t)\rangle_{CA}=-\frac{\alpha_2 n_C^0}{2k'u}\left[Z\left[\frac{a+i\gamma}{k'u}\right]-\exp[-(\gamma-ia)t-\tfrac{1}{4}k'^2u^2t^2]Z\left[\frac{a+i\gamma}{k'u}+\tfrac{1}{2}ik'ut\right]\right]^* , \tag{7.9}$$

where $Z(\xi)$ is the plasma-dispersion function,

$$k'=|k_2+\tfrac{1}{2}k_1| \ , \ \ \gamma=\tfrac{1}{2}(\Gamma_3+\Gamma_1)$$

(recall $\Gamma_1=\Gamma_2$), and $a=\Delta_{32}+\alpha_1+\frac{1}{2}\Delta_{21}$. The time-dependent part in (7.9) disappears in a characteristic time $\min[(k'u)^{-1},\gamma^{-1}]$. If $k'u>>\gamma$, velocity dephasing is the dominant decay mechanism; in the case $k'u<<\gamma$, the system behaves as a homogeneous one decaying at a rate γ and oscillating with a frequency $(\Delta_{32}+\alpha_1+\frac{1}{2}\Delta_{21})$.

In a second example, field α_2 is kept constant and α_1 is switched on at $t=0$. The probe response reflects the decay of the initial $\widetilde{\rho}_{BA}$ coherence (recall that $\widetilde{\rho}_{AA}^0$ and $\widetilde{\rho}_{BB}^0$ remain unchanged). Assuming that (7.5) is valid, we obtain from (7.6)

$$\begin{aligned}\widetilde{\rho}_{CA}(t)=\widetilde{\rho}_{CA}(0)e^{-(\gamma_{CA}+i\omega_{CA})t}&-\frac{i\alpha_2\sin\theta(n_C^0-n_A^0)}{\gamma_{CA}+i\omega_{CA}}(1-e^{-(\gamma_{CA}+i\omega_{CA})t})\\ &-\frac{i\alpha_2(n_1^0-n_2^0)\sin2\theta\cos\theta}{2(\gamma_{CA}-\gamma+i\omega_{CB})}(e^{-(\gamma+i\omega_{BA})t}-e^{-(\gamma_{CA}+i\omega_{CA})t}) ,\end{aligned} \tag{7.10a}$$

$$\begin{aligned}\widetilde{\rho}_{CB}(t)=\widetilde{\rho}_{CB}(0)e^{-(\gamma_{CB}+i\omega_{CB})t}&+\frac{i\alpha_2\cos\theta(n_C^0-n_B^0)}{\gamma_{CB}+i\omega_{CB}}(1-e^{-(\gamma_{CB}+i\omega_{CB})t})\\ &+\frac{i\alpha_2(n_1^0-n_2^0)\sin2\theta\sin\theta}{2(\gamma_{CB}-\gamma+i\omega_{CA})}(e^{-(\gamma-i\omega_{BA})t}-e^{-(\gamma_{CB}+i\omega_{CB})t}) ,\end{aligned} \tag{7.10b}$$

with initial conditions

$$\widetilde{\rho}_{CA}(0)=-i\alpha_2\sin\theta(n_3^0-n_2^0)(\gamma_{32}+i\widetilde{\Delta}_{32})^{-1} , \tag{7.11a}$$

$$\widetilde{\rho}_{CB}(0)=i\alpha_2\cos\theta(n_3^0-n_2^0)(\gamma_{32}+i\widetilde{\Delta}_{32})^{-1} . \tag{7.11b}$$

The assumption $\Gamma_1=\Gamma_2=\gamma$ implies that $\gamma_{CB}=\gamma_{CA}=\frac{1}{2}\Gamma_3+\frac{1}{2}\gamma$.

The velocity averaging of (7.10) is by no means easy except in the special cases when ω_{CA} or ω_{CB} is nearly independent of v (Doppler-free cases). The labeling of the various terms in (7.10) is obvious: The first term gives the decay of the initial coherence, the second one describes the transient to the new steady state, and the third one is due to the decay of the initial $\widetilde{\rho}_{BA}$ coherence (nutation in the 1↔2 system). The various terms in Eqs. (7.10) can be isolated by a proper choice of experimental parameters [e.g., by choosing α_1 such that $n_C^0=n_A^0$ the second term in Eq. (7.10a) can be eliminated].

The advantage of the DAP over the BAP is that the DAP gives directly the correct eigenfrequencies ω_{CB} and ω_{CA} (in the BAP one is required to fully solve the problem using Laplace-transform techniques[71] to obtain these values).

VIII. CONCLUSION

The DAP offers little computational advantage over the BAP for most calculations. However, when the frequency separations of the dressed states are much greater than the relaxation rates of these states, the equations of the DAP simplify considerably. In this case, it appears that the dressed basis is the natural one in which to do calculations. Interpretations of the results in both the stationary and transient regime are straightforward in this representation. The positions of the resonances in saturation spectroscopy as well as the oscillation frequencies observable in coherent transient experiments appear as fundamental parameters in the DAP.

When the relaxation rates are comparable with the field strengths, the BAP is generally an easier representation to use than the DAP. In some cases it may be difficult to interpret the results obtained using the BAP in terms of fundamental physical processes, but the calculations needed to arrive at these results are much more readily done in the BAP. Moreover, the BAP has the advantage of directly supplying the physical observables.

The DAP may be useful when applied to the analysis of atom-field interactions involving multilevel atoms or multimode fields. It also seems to be a convenient basis to use in solving coherent transient problems of the type discussed in Sec. VII.

ACKNOWLEDGMENTS

We would like to thank Prof. C. Cohen-Tannoudji for discussing various aspects of the DAP with us. This work was stimulated by the Klosk lectures given by Prof. Cohen-Tannoudji at New York University in February 1981. R. S. wishes to acknowledge the hospitality of New York University during his stay. The research is supported by the U. S. Office of Naval Research.

APPENDIX A: RELAXATION SCHEME IN THE DAP

The relaxational coupling and decay in the DAP is obtained by transforming the relaxation terms of the BAP, Eq. (2.19), with the aid of (2.8), (2.11), and (2.17). To slightly simplify the equations we assume $\Gamma_{13}=\Gamma_{31}=0$ (no collisional mixing of states 1 and 3), and find for the nonvanishing diagonal elements

$$R_{AA,AA}=-\Gamma_1\cos^2\theta-\Gamma_2\sin^2\theta-\tfrac{1}{4}(\varphi-\Gamma_{12}-\Gamma_{21})\sin^2 2\theta\ , \tag{A1a}$$

$$R_{AA,BB}=\tfrac{1}{4}\varphi\sin^2 2\theta+\Gamma_{12}\sin^4\theta+\Gamma_{21}\cos^4\theta\ , \tag{A1b}$$

$$R_{AA,CC}=\Gamma_{32}\sin^2\theta\ , \tag{A1c}$$

$$R_{AA,AB}=R_{AA,BA}=\tfrac{1}{4}\sin 2\theta(\Gamma_2-\Gamma_1+\varphi\cos 2\theta-2\Gamma_{21}\cos^2\theta+2\Gamma_{12}\sin^2\theta)\ , \tag{A1d}$$

$$R_{BB,AA}=\tfrac{1}{4}\varphi\sin^2 2\theta+\Gamma_{12}\cos^4\theta+\Gamma_{21}\sin^4\theta\ , \tag{A2a}$$

$$R_{BB,BB}=-\Gamma_1\sin^2\theta-\Gamma_2\cos^2\theta-\tfrac{1}{4}(\varphi-\Gamma_{12}-\Gamma_{21})\sin^2 2\theta\ , \tag{A2b}$$

$$R_{BB,CC}=\Gamma_{32}\cos^2\theta\ , \tag{A2c}$$

$$R_{BB,AB}=R_{BB,BA}=\tfrac{1}{4}\sin 2\theta(\Gamma_2-\Gamma_1-\varphi\cos 2\theta+2\Gamma_{12}\cos^2\theta-2\Gamma_{21}\sin^2\theta)\ , \tag{A2d}$$

$$R_{CC,CC}=-\Gamma_3\ , \tag{A3a}$$

$$R_{CC,AA}=\Gamma_{23}\sin^2\theta\ , \tag{A3b}$$

$$R_{CC,BB}=\Gamma_{23}\cos^2\theta\ , \tag{A3c}$$

$$R_{CC,AB}=R_{CC,BA}=-\tfrac{1}{2}\Gamma_{23}\sin 2\theta\ , \tag{A3d}$$

where

$$\varphi=2\gamma_{21}-\Gamma_1-\Gamma_2 \tag{A4}$$

gives a measure of the effect of phase-changing collisions. The nonvanishing terms involved in the off-diagonal elements are given by

$$R_{BA,BA}=-\gamma_{21}+\tfrac{1}{4}(\varphi-\Gamma_{12}-\Gamma_{21})\sin^2 2\theta\ , \tag{A5a}$$

$$R_{BA,AB}=\tfrac{1}{4}(\varphi-\Gamma_{12}-\Gamma_{21})\sin^2 2\theta\ , \tag{A5b}$$

$$R_{BA,AA}=\tfrac{1}{4}\sin 2\theta(\Gamma_2-\Gamma_1+\varphi\cos 2\theta+2\Gamma_{21}\sin^2\theta-2\Gamma_{12}\cos^2\theta)\ , \tag{A5c}$$

$$R_{BA,BB}=\tfrac{1}{4}\sin 2\theta(\Gamma_2-\Gamma_1-\varphi\cos 2\theta+2\Gamma_{21}\cos^2\theta-2\Gamma_{12}\sin^2\theta)\ , \tag{A5d}$$

$$R_{BA,CC}=-\tfrac{1}{2}\Gamma_{32}\sin 2\theta\ , \tag{A5e}$$

$$R_{CA,CA}=-\gamma_{31}\cos^2\theta-\gamma_{32}\sin^2\theta\ , \tag{A6}$$

$$R_{CB,CB}=-\gamma_{31}\sin^2\theta-\gamma_{32}\cos^2\theta\ , \tag{A7}$$

$$R_{CA,CB}=R_{CB,CA}=\tfrac{1}{2}(\gamma_{32}-\gamma_{31})\sin 2\theta\ , \tag{A8}$$

with the remaining elements given by the symmetry property $R_{\alpha\beta,\sigma\delta}=R_{\beta\alpha,\delta\sigma}$. Note that either Γ_{ij} or Γ_{ji}, depending on the configuration, vanishes if states i and j are not mixed by collisions. When phase-changing collisions are absent, i.e., $\gamma_{ij}=\frac{1}{2}(\Gamma_i+\Gamma_j)$, and all $\Gamma_{ij}=0$, the relaxation terms are those given in (2.23). In a general case all the terms (A1)–(A8) differ from zero, leading to a complicated relaxation scheme in the DAP.

APPENDIX B: PROBE AND SATURATOR RESPONSES

The solution of Eqs. (2.22) to zeroth order in α_2 is given by

$$\tilde{\rho}^0_{11}=n^0_1+\frac{2\alpha_1^2}{\Gamma_1}\gamma_{21}n^0_{21}(\tilde{\Delta}^2_{21}+\Gamma^2)^{-1}\ , \tag{B1a}$$

$$\tilde{\rho}^0_{22}=n^0_2-\frac{2\alpha_1^2}{\Gamma_2}\gamma_{21}n^0_{21}(\tilde{\Delta}^2_{21}+\Gamma^2)^{-1}\ , \tag{B1b}$$

$$\tilde{\rho}^0_{33}=n^0_3\ , \tag{B1c}$$

$$\tilde{\rho}^0_{21}=i\alpha_1 n^0_{21}(\gamma_{21}-i\tilde{\Delta}_{21})(\tilde{\Delta}^2_{21}+\Gamma^2)^{-1}\ , \tag{B1d}$$

where $n_i^0=\Lambda_i/\Gamma_i$, $n^0_{21}=n^0_2-n^0_1$, and

$$\Gamma^2=\gamma_{21}^2+2\alpha_1^2\gamma_{21}(\Gamma_1^{-1}+\Gamma_2^{-1})$$
$$=\tfrac{1}{4}(\Gamma_1+\Gamma_2)^2(1+4\alpha_1^2/\Gamma_1\Gamma_2) \tag{B2}$$

[the last step follows from the assumption $\gamma_{21}=\frac{1}{2}(\Gamma_1+\Gamma_2)$]. The components $\tilde{\rho}^0_{32}$ and $\tilde{\rho}^0_{31}$ vanish. The corresponding DAP equations read

$$\tilde{\rho}^0_{AA}=n^0_A+\frac{2\beta^2}{\Gamma_A}\gamma_{BA}n^0_{BA}(\omega^2_{BA}+\Gamma^2_{BA})^{-1}\ , \tag{B3a}$$

$$\tilde{\rho}^0_{BB}=n^0_B+\frac{2\beta^2}{\Gamma_B}\gamma_{BA}n^0_{BA}(\omega^2_{BA}+\Gamma^2_{BA})^{-1}\ , \tag{B3b}$$

$$\tilde{\rho}^0_{CC}=n^0_C\ , \tag{B3c}$$

$$\tilde{\rho}^0_{BA}=\beta n^0_{BA}(\gamma_{BA}-i\omega_{BA})(\omega^2_{BA}+\Gamma^2_{BA})^{-1}\ , \tag{B3d}$$

where $n^0_\alpha=\Lambda_\alpha/\Gamma_\alpha$,

$$n^0_{BA}=n^0_B+n^0_A+\Lambda_{BA}/\beta\ , \tag{B4a}$$

$$\Gamma^2_{BA}=\gamma^2_{BA}-2\beta^2\gamma_{BA}(\Gamma_A^{-1}+\Gamma_B^{-1})=\tfrac{1}{4}(\Gamma_B+\Gamma_A)^2(1-4\beta^2/\Gamma_A\Gamma_B)\ , \tag{B4b}$$

and β is defined by Eq. (2.27). In terms of the BAP variables, the "population inversion" n^0_{BA} and the effective width Γ_{BA} can be written as

$$n^0_{BA}=-\frac{\Gamma_2+\Gamma_1}{\Gamma_2-\Gamma_1}n^0_{21}\left[1+\frac{(\Gamma_2-\Gamma_1)^2}{4\Gamma_1\Gamma_2}\sin^2 2\theta\right]^{-1}\ , \tag{B5a}$$

$$\Gamma^2_{BA}=\tfrac{1}{4}(\Gamma_1+\Gamma_2)^2\left[1+\frac{(\Gamma_2-\Gamma_1)^2}{4\Gamma_1\Gamma_2}\sin^2 2\theta\right]^{-1}\ . \tag{B5b}$$

[Notice that n^0_{BA} enters only in the product βn^0_{BA} which is nonsingular for $(\Gamma_1-\Gamma_2)=0$.]

To first order in α_2 we find from (2.22e) and (2.22f)

$$\tilde{\rho}_{32}=i\alpha_2\frac{[\gamma_{31}+i(\tilde{\Delta}_{32}+\tilde{\Delta}_{21})](\tilde{\rho}^0_{33}-\tilde{\rho}^0_{22})-i\alpha_1\tilde{\rho}^0_{21}}{[\gamma_{31}+i(\tilde{\Delta}_{32}+\tilde{\Delta}_{21})](\gamma_{32}+i\tilde{\Delta}_{32})+\alpha_1^2}\ . \tag{B6}$$

In the DAP we obtain from (2.23d), and (2.23e)

$$\tilde{\rho}_{CA}=-i\alpha_2\{(\gamma_{CB}+i\omega_{CB})[\sin\theta(\tilde{\rho}^0_{CC}-\tilde{\rho}^0_{AA})+\cos\theta\tilde{\rho}^0_{BA}]$$
$$-\beta[\cos\theta(\tilde{\rho}^0_{CC}-\tilde{\rho}^0_{BB})+\sin\theta\tilde{\rho}^0_{AB}]\}[(\gamma_{CA}+i\omega_{CA})(\gamma_{CB}+i\omega_{CB})-\beta^2]^{-1}\ , \tag{B7a}$$

$$\tilde{\rho}_{CB}=i\alpha_2\{(\gamma_{CA}+i\omega_{CA})[\cos\theta(\tilde{\rho}^0_{CC}-\tilde{\rho}^0_{BB})+\sin\theta\tilde{\rho}^0_{AB}]$$
$$-\beta[\sin\theta(\tilde{\rho}^0_{CC}-\tilde{\rho}^0_{AA})+\cos\theta\tilde{\rho}^0_{BA}]\}[(\gamma_{CA}+i\omega_{CA})(\gamma_{CB}+i\omega_{CB})-\beta^2]^{-1}\,, \tag{B7b}$$

which after insertion into (2.29e) yield the observable $\tilde{\rho}_{32}$. The DAP solution Eq. (B7) is clearly much more complicated than the BAP expression (B6).

The DAP solution simplifies considerably in the limit $\omega_{BA} >> \gamma_{BA},\Gamma_{BA}$. The lowest-order terms are given by

$$\tilde{\rho}^0_{\alpha\alpha}=n^0_\alpha+O(\gamma^2/\omega^2_{BA})\,, \tag{B8a}$$

$$\tilde{\rho}^0_{BA}=-i\beta n^0_{BA}/\omega_{BA}+O(\gamma^2/\omega^2_{BA})\,. \tag{B8b}$$

[The corresponding solutions in the BAP would be

$$\tilde{\rho}^0_{ii}=n^0_i,\ \tilde{\rho}^0_{21}=i\alpha_1 n^0_{21}/(\gamma_{21}+i\Delta_{21})\,,$$

according to (B1).] As $\beta\simeq\gamma$ we see that $\tilde{\rho}^0_{BA}$ is roughly a factor γ/ω_{BA} smaller than the diagonal elements $\tilde{\rho}^0_{\alpha\alpha}$. The rate-type solution (3.2) is obtained by neglecting $\tilde{\rho}^0_{BA}$ and terms proportional to β in (B7). This approximation is equivalent to keeping only the lowest-order terms in a power expansion in terms of γ/ω_{BA}. In the following, we study in some detail the accuracy of (3.2).

Strongly coupled transition 1↔2

If we insert (B8) into (2.29), we obtain, after going back to the BAP variables,

$$\tilde{\rho}^0_{11}\simeq n^0_1+\frac{2\alpha_1^2}{\Gamma_1}\gamma_{21}n^0_{21}(\tilde{\Delta}^2_{21}+4\gamma^2_{21}\alpha^2_1/\Gamma_1\Gamma_2)^{-1}\,, \tag{B9a}$$

$$\tilde{\rho}^0_{22}\simeq n^0_2-\frac{2\alpha_1^2}{\Gamma_2}\gamma_{21}n^0_{21}(\tilde{\Delta}^2_{21}+4\gamma^2_{21}\alpha^2_1/\Gamma_1\Gamma_2)^{-1}\,, \tag{B9b}$$

$$\tilde{\rho}^0_{21}\simeq i\alpha_1 n^0_{21}(\gamma_{21}-i\tilde{\Delta}_{21})(\tilde{\Delta}^2_{21}+4\gamma^2_{21}\alpha^2_1/\Gamma_1\Gamma_2)^{-1}\,. \tag{B9c}$$

A comparison between (B1) and (B9) reveals that the approximation is good provided that

$$\tilde{\Delta}^2_{21}+4\alpha^2_1\gamma^2_{21}/\Gamma_1\Gamma_2>>\gamma^2_{21}\,. \tag{B10}$$

This condition is satisfied when either $|\tilde{\Delta}_{21}| >> \gamma_{21}$ or $\alpha_1^2>>\frac{1}{4}\Gamma_1\Gamma_2$. Note that if we neglect (B8b) there is no absorption of the strong field α_1 [the first term in (2.29d) is real and describes dispersion only].

Probe response

We can express the exact result (B6) in a form[13]

$$\tilde{\rho}_{32}=i\alpha_2[W_+(Z_++i\tilde{\Delta}_{32})^{-1}+W_-(Z_-+i\tilde{\Delta}_{32})^{-1}]\,, \tag{B11}$$

where

$$Z_\pm=\tfrac{1}{2}(\gamma_{32}+\gamma_{31}+i\tilde{\Delta}_{21})\mp\tfrac{1}{2}i[(\tilde{\Delta}_{21}+i\gamma_{32}-i\gamma_{31})^2+4\alpha_1^2]^{1/2}\,, \tag{B12}$$

$$W_\pm=\tfrac{1}{2}(\tilde{\rho}^0_{33}-\tilde{\rho}^0_{22})\pm[\tfrac{1}{2}(\tilde{\rho}^0_{33}-\tilde{\rho}^0_{22})(\tilde{\Delta}_{21}+i\gamma_{32}-i\gamma_{31})-\alpha_1\tilde{\rho}^0_{21}][(\tilde{\Delta}_{21}+i\gamma_{32}-i\gamma_{31})^2+4\alpha_1^2]^{-1/2}\,. \tag{B13}$$

An expansion of (B12) and (B13) in terms of the assumedly small parameter

$$\epsilon=(\gamma_{32}-\gamma_{31})/(\tilde{\Delta}^2_{21}+4\alpha^2_1)^{1/2} \tag{B14}$$

yields

$$Z_++i\tilde{\Delta}_{32}\simeq\gamma_{CB}+\tfrac{1}{4}\alpha_1\sin4\theta\epsilon^3+i\omega_{CB}+\tfrac{1}{2}i\alpha_1\sin2\theta\epsilon^2\,, \tag{B15a}$$

$$Z_-+i\tilde{\Delta}_{32}\simeq\gamma_{CA}-\tfrac{1}{4}\alpha_1\sin4\theta\epsilon^3+i\omega_{CA}-\tfrac{1}{2}i\alpha_1\sin2\theta\epsilon^2\,, \tag{B15b}$$

$$W_+ \simeq (n_C^0 - n_B^0)\cos^2\theta + \tfrac{1}{2} i\epsilon \sin^2 2\theta n_C^0 + \tfrac{1}{4} i \sin^2 2\theta(\Lambda_1 - \Lambda_2)/\omega_{BA} \,, \tag{B16a}$$

$$W_- \simeq (n_C^0 - n_A^0)\sin^2\theta - \tfrac{1}{2} i\epsilon \sin^2 2\theta n_C^0 - \tfrac{1}{4} i \sin^2 2\theta(\Lambda_1 - \Lambda_2)/\omega_{BA} \,. \tag{B16b}$$

A finite value of ϵ slightly changes the widths and positions of the resonances. The corrections are negligible when $(\widetilde{\Delta}_{21}^2 + 4\alpha_1^2)^{1/2} >> \frac{1}{2}|\Gamma_1 - \Gamma_2|$ which is a relatively mild condition. The expressions (B16) for the weight factors $W_\pm$ are accurate to order $O(\epsilon^2;\epsilon\gamma/\omega_{BA};\gamma^2/\omega_{BA}^2)$ and coincide with those given in (3.2) provided that $|\epsilon| << 1$ and

$$|n_C^0 - n_B^0| >> |\Lambda_1 - \Lambda_2| \sin^2\theta/\omega_{BA} \,, \tag{B17a}$$

$$|n_C^0 - n_A^0| >> |\Lambda_1 - \Lambda_2| \cos^2\theta/\omega_{BA} \,. \tag{B17b}$$

The correction terms given in (B16) are purely imaginary and, therefore, introduce a dispersive-type change in the absorption spectrum ($\sim \mathrm{Im}\widetilde{\rho}_{32}$). This change causes a small shift in the position of the resonances, but does not appreciably affect their height.

APPENDIX C: DOPPLER-BROADENED PROBE SPECTRA

Introducing the dimensionless parameters (5.3)–(5.6) into (5.2) and solving the equations $\omega_C = \omega_{A,B}$ for x, we obtain

$$x_{1,2} = -\frac{k_1(2k_2+k_1)}{2k_2(k_1+k_2)}\nu \pm \frac{k_1^2}{2k_2(k_1+k_2)}\left[\nu^2 + \frac{4k_2(k_1+k_2)}{k_1^2}\right]^{1/2} . \tag{C1}$$

If $k_2(k_1+k_2) > 0$, both the roots in (C1) are real. The root with the plus (minus) sign satisfies the CB (CA) resonance condition when $k_2 > 0$ ($k_2 < 0$). If $k_2(k_1+k_2) < 0$, $x_{1,2}$ are complex in the region (5.10); otherwise both roots belong to the branch $\omega_{CB} = 0$ for $\nu > \nu_{\mathrm{cr}} > 0$ and to the branch $\omega_{CA} = 0$ when $\nu < -\nu_{\mathrm{cr}}$. In all cases the solutions (C1) must fall within the Doppler profile [see Eq. (5.9)] so that the Doppler-distribution function is not negligibly small.

Case $k_2(k_1+k_2) > 0$

Inserting (C1) into (5.8), we obtain after lengthy algebraic manipulations

$$\begin{aligned} I(\nu) = \frac{\pi}{2|k_2|} W(v_{CB}) \Bigg[(n_3^0 - n_2^0)\left[1 - \frac{\nu\,\mathrm{sgn}(k_2)}{[\nu^2 + 4k_2(k_1+k_2)/k_1^2]^{1/2}}\right] + (n_2^0 - n_1^0)\frac{|k_2|}{k_1\Gamma_2}\frac{\gamma_{\mathrm{eff}}}{\nu^2 + \gamma_{\mathrm{eff}}^2/\Gamma_1\Gamma_2} \\ \times \left[1 - \frac{\nu[k_2\Gamma_1 - (k_1+k_2)\Gamma_2]/k_1\gamma_{\mathrm{eff}}}{[\nu^2 + 4k_2(k_1+k_2)/k_1^2]^{1/2}}\right]\Bigg] + \frac{\pi}{2|k_2|} W(v_{CA})[\nu \to -\nu] \,, \end{aligned} \tag{C2}$$

where $\omega_{CB}(v_{CB}) = 0$, $\omega_{CA}(v_{CA}) = 0$, and where γ_{eff} is defined by (5.12). Provided that

$$\left[\nu^2 + \frac{4k_2(k_1+k_2)}{k_1^2}\right] \left|\nu + \frac{2k_2(k_1+k_2)\Delta_{21}}{k_1(2k_2+k_1)\alpha_1}\right| << \frac{k_2^2(k_1+k_2)^2u^2}{k_1|2k_2+k_1|\alpha_1^2} \tag{C3}$$

the Gaussians in (C2) are approximately equal,

$$W(v_{CA}) \simeq W(v_{CB}) \simeq \exp\left[-\left[\frac{\Delta_{32}}{k_2} + \frac{\Delta_{32}+\Delta_{21}}{k_1+k_2}\right]^2 \Big/ 4u^2\right] \Big/ \pi^{1/2}u \tag{C4}$$

and the simple result given in the text, Eq. (5.11), is valid. When (C3) is violated the dominant structure in the absorption spectrum arises from the Gaussians, and Eqs. (5.14) and (5.16) become applicable.

Case $k_2(k_1+k_2) < 0$

If $\nu > \nu_{\mathrm{cr}} > 0$, both of the roots (C1) satisfy the equation $\omega_{CB} = 0$ (if $\nu < -\nu_{\mathrm{cr}}$ the equation $\omega_{CA} = 0$). Thus only the *CB* transition contributes, and we can approximate

$$\tilde{\rho}_{32} \simeq i\alpha_2 \cos^2\theta (n_C^0 - n_B^0)(\gamma_{CB} + i\omega_{CB})^{-1} . \tag{C5}$$

This can be written as

$$\tilde{\rho}_{32} \simeq -\frac{\alpha_2}{\gamma_{CB}} g(x) \cos^2\theta (n_C^0 - n_B^0)[(x-x_1)(x-x_2)+ig(x)]^{-1} , \tag{C6}$$

where

$$g(x) = -\frac{\gamma_{CB} k_1^2}{\alpha_1 k_2 (k_1+k_2)} \left[\nu + \left[\frac{k_2}{k_1} + \frac{1}{2} \right] x + \tfrac{1}{2}(x^2+4)^{1/2} \right] . \tag{C7}$$

The last factor can be expanded as

$$\begin{aligned} \operatorname{Im}\{[(x-x_1)(x-x_2)+ig]^{-1}\} \simeq \operatorname{Im} \Bigg[& [(x_2-x_1)^2+4ig]^{-1/2} \\ & \times \left[\mathscr{P}\frac{1}{x-x_1} - i\pi\delta(x-x_1) - \mathscr{P}\frac{1}{x-x_2} - i\pi\delta(x-x_2) \right] \Bigg] , \end{aligned} \tag{C8}$$

where the complex square root has to be evaluated so that its imaginary part is positive (assume $x_2 > x_1$). The principal values in (C8) are negligible, because for $(x_2 - x_1) >> \gamma/\alpha_1$ the complex square root is real and for $x_2 \simeq x_1$ they cancel. Inserting (C8) into (C6), we obtain

$$\begin{aligned} I_{CB}(\nu) \simeq \frac{k_1 \pi^{1/2}}{|k_2|\,|k_1+k_2|\,u} \sum_{i=1}^{2} \exp & \left[- \left[\frac{\alpha_1 x_i - \Delta_{21}}{k_1 u} \right]^2 \right] \\ & \times [n_C^0 - n_B^0(x_i)] \left[\nu + \frac{k_1+k_2}{k_1} x_i \right] \operatorname{Re}\{[(x_2-x_1)^2 + 4ig(x_i)]^{-1/2}\} . \end{aligned} \tag{C9}$$

In the limit $x_2 \rightarrow x_1$, this gives, after insertion of the explicit expressions (C1) for x_1 and x_2

$$\begin{aligned} I_{CB}(\nu) \simeq & \frac{1}{k_1 u} \left[\frac{2\pi(k_1+k_2)}{|k_2|} \right]^{1/2} \left[(n_3^0 - n_2^0) + \frac{\Gamma_1 |k_2|}{\Gamma_1 |k_2| + \Gamma_2 |k_1+k_2|} (n_2^0 - n_1^0) \right] \\ & \times \exp\left[- \left[\Delta_{21} - \alpha_1 \frac{k_1+2k_2}{(|k_2(k_1+k_2)|)^{1/2}} \right]^2 \Big/ k_1^2 u^2 \right] \\ & \times \operatorname{Re}\left\{ \left[\nu - \nu_{\text{cr}} - \frac{i}{\alpha_1} \left[\frac{|k_2|}{k_1}\gamma_{31} + \frac{k_1+k_2}{k_1}\gamma_{32} \right] \right]^{-1/2} \right\} , \end{aligned} \tag{C10}$$

when $x_2 - x_1 >> \gamma/\alpha_1$, Eq. (C9) reduces to

$$\begin{aligned} I(\Delta_{32}) \simeq & \frac{\pi^{1/2}}{2|k_2|u} \exp\left[- \left[\frac{\alpha_1 x_2 - \Delta_{21}}{k_1 u} \right]^2 \right] \\ & \times \Bigg\{ (n_3^0 - n_2^0) \left[1 + \frac{\nu}{(\nu^2 - \nu_{\text{cr}}^2)^{1/2}} \right] \\ & \quad + (n_2^0 - n_1^0) \frac{k_2}{k_1^2 \Gamma_2} \left[\Gamma_1 k_2 \left[1 + \frac{\nu}{(\nu^2-\nu_{\text{cr}}^2)^{1/2}} \right] + \Gamma_2 (k_1+k_2) \left[1 - \frac{\nu}{(\nu^2-\nu_{\text{cr}}^2)^{1/2}} \right] \right] \\ & \quad \times \left[\nu^2 + \left[\Gamma_1 \frac{k_2}{k_1} + \Gamma_2 \frac{k_1+k_2}{k_1} \right]^2 \frac{1}{\Gamma_1 \Gamma_2} \right]^{-1} \Bigg\} + \text{term}[(\nu^2-\nu_{\text{cr}}^2)^{1/2} \rightarrow -(\nu^2-\nu_{\text{cr}}^2)^{1/2}] . \end{aligned} \tag{C11}$$

In the limit $\nu \rightarrow \infty$, (C11) gives just the flat background absorption. Both (C10) and (C11) agree with the limiting intense-field results given in Ref. 13.

*Permanent address: Technical Research Centre of Finland, SF 02150 Espoo 15, Finland.

[1] *Laser Spectroscopy III,* edited by J. L. Hall and J. L. Carlsten (Springer, New York, 1977). This reference, as well as Refs. 2–6 below, contain many review articles in the general area of laser spectroscopy.

[2] *Laser Spectroscopy IV,* edited by H. Walther and K. W. Rothe (Springer, Berlin, 1979).

[3] *High Resolution Laser Spectroscopy,* edited by K. Shimoda (Springer, New York, 1976).

[4] *Laser Spectroscopy of Atoms and Molecules,* edited by H. Walther (Springer, New York, 1976).

[5] V. S. Letokhov and V. P. Chebotaev, *Non-Linear Laser Spectroscopy* (Springer, New York, 1977).

[6] *Frontiers in Laser Spectroscopy,* edited by R. Balian, S. Haroche, and S. Liberman (North-Holland, Amsterdam, 1977).

[7] G. E. Notkin, S. G. Rautian, and A. A. Feoktistov, Zh. Eksp. Teor. Fiz. 52, 1673 (1967) [Sov. Phys.—JETP 25, 1112 (1967)].

[8] M. S. Feld and A. Javan, Phys. Rev. 177, 540 (1969).

[9] T. W. Hänsch and P. E. Toschek, Z. Phys. 236, 213 (1970).

[10] S. Haroche and F. Hartmann, Phys. Rev. A 6, 1280 (1972).

[11] I. M. Beterov and V. P. Chebotaev, Prog. Quantum Electron. 3, 1 (1974), and references therein.

[12] R. M. Whitley and C. R. Stroud, Phys. Rev. A 14, 1498 (1976).

[13] R. Salomaa and S. Stenholm, J. Phys. B 8, 1795 (1975); 9, 1221 (1976).

[14] R. Salomaa, J. Phys. B 10, 3005 (1977).

[15] R. Salomaa, Physica Ser. 15, 251 (1977).

[16] C. J. Borde in Ref. 1, p. 121.

[17] C. Delsart and J. C. Keller, J. Phys. (Paris) 39, 350 (1978).

[18] P. R. Berman, P. F. Liao, and J. E. Bjorkholm, Phys. Rev. A 20, 2389 (1979).

[19] C. Cohen-Tannoudji and S. Reynaud, J. Phys. B 10, 345 (1977); 10, 365 (1977).

[20] C. Cohen-Tannoudji and S. Reynaud, J. Phys. B 10, 2311 (1977).

[21] S. Reynaud, thesis, University of Paris, 1977 (unpublished).

[22] F. Hoffbeck, thesis, University of Paris, 1978 (unpublished).

[23] E. Arimondo and P. Glorieux, Phys. Rev. A 19, 1067 (1979).

[24] M. Himbert, thesis, University of Paris, 1980 (unpublished).

[25] See, for example, A. Ben Reuven and L. Klein, Phys. Rev. A 4, 753 (1971); L. Klein, M. Giraud and A. Ben Reuven, *ibid.* 10, 682 (1974); Y. Rabin and A. Ben Reuven, J. Phys. B 13, 2011 (1980).

[26] C. Cohen-Tannoudji, in *Cargese Lectures in Physics* (Gordon and Breach, New York, 1968), Vol. 2, p. 347.

[27] G. Nienhuis and F. Schuller, J. Phys. B 12, 3473 (1979).

[28] Neglect terms of order $|\Omega_2-|\omega_{32}||/(\Omega_2+|\omega_{32}|)$ and $|\Omega_1-|\omega_{21}||/|\Omega_1+|\omega_{21}||$.

[29] Our field interaction representation is defined by

$$\tilde{\rho}_{21}=\rho_{21}\exp[i\,\mathrm{sgn}(\omega_{21})(\Omega_1 t-K_1 z+\varphi_1)]\ ,$$

$$\tilde{\rho}_{32}=\rho_{32}\exp[i\,\mathrm{sgn}(\omega_{32})(\Omega_2 t-K_2 z+\varphi_2)]\ ,$$

$$\tilde{\rho}_{31}=\rho_{31}\exp[\,i\,\mathrm{sgn}(\omega_{21})(\Omega_1 t-K_1 z+\varphi_1)+i\,\mathrm{sgn}(\omega_{32})(\Omega_2 t-K_2 z+\varphi_2)]\ ,$$

$$\tilde{\rho}_{ii}=\rho_{ii}\ .$$

[30] In a more general case, the relaxation is described by an integral equation to account for velocity-changing collisions. See, for example, P. R. Berman, Phys. Rep. 43, 101 (1978).

[31] M. Lax, Phys. Rev. 172, 350 (1968). B. R. Mollow, Phys. Rev. A 12, 1919 (1975), and references therein; A. V. Kruglikov, Opt. Spektrosk. 47, 1033 (1979) [Opt. Spectrosc. (USSR) 47, 573 (1979)]; G. Nienhuis and F. Schuller, J. Phys. B 13, 2205 (1980).

[32] The power absorption coefficient of the probe wave (in units of m^{-1}) is obtained by multiplying $I(\Delta_{32})$ by a factor $(\Omega_2\mu_{32}^2/\hbar c\epsilon_0)$. A positive value of $I(\Delta_{32})$ indicates that there is probe gain in the V and cascade configurations and probe absorption in the Λ configuration.

[33] See Fig. 5 of Ref. 18.

[34] Recall that our rate-type approximation is valid provided

$$\omega_{BA}=[(\Delta_{21}+k_1 v)^2+4\alpha_1^2]^{1/2}>2\alpha_1>>\Gamma\ .$$

[35] The plasma-dispersion function is defined by

$$Z(\psi)=\pi^{-1/2}\int_{-\infty}^{\infty}dt\,\exp(-t^2)(t-\psi)^{-1}$$

with $\mathrm{Im}\psi>0$; it may be related to the complex error function.

[36] For reviews of this subject, see, G. Grynberg and B. Cagnac, Rep. Prog. Phys. 40, 791 (1977); and M. Salour, Rev. Mod. Phys. 50, 667 (1978).

[37] K. Shimoda, Appl. Phys. (Germany) 9, 239 (1976).

[38] M. F. H. Schuurmans, Phys. Lett. A63, 25 (1977).

[39] R. L. Panock and R. J. Temkin, IEEE J. Quantum Electron. QE 13, 425 (1977).

[40] B. Sobolewska, Opt. Commun. 20, 378 (1977).

[41] C. Mavroyannis, Opt. Commun. 29, 80 (1979).

[42] Z. Bialynicka-Birula and I. Bialynicki-Birula, Phys. Rev. A 16, 1318 (1977).

[43] S. J. Petuchowski, J. D. Oberstar, and T. A. DeTemple, Phys. Rev. A 20, 529 (1979).

[44] D. J. Kim and P. D. Coleman, IEEE J. Quantum Electron. QE 16, 300 (1980).

[45] If $k_D(k_D+k_1)(k_D-k_2)=0$ (or if either $\alpha_1^2=0$ or $\alpha_2^2=0$), Eq. (6.1) with $\omega=\Delta_D+k_D v$ reduces to a second-order equation in v, and the analysis is as in Sec. V.

[46] S. G. Rautian and I. I. Sobelman, Zh. Eksp. Teor. Fiz. 44, 934 (1963) [Sov. Phys.—JETP 17, 635 (1963)].

(1963)].

[47] B. J. Feldman and M. S. Feld, Phys. Rev. A 5, 899 (1972).

[48] N. Skribanowitz, M. J. Kelly, and M. S. Feld, Phys. Rev. A 6, 2302 (1972).

[49] E. V. Baklanov, I. M. Beterov, B. Ya. Dubetskii, and V. P. Chebotaev, Pis'ma Zh. Eksp. Teor. Fiz. 22, 289 (1975) [Sov. Phys.—JETP Lett. 22, 134 (1975)].

[50] P. R. Berman and J. Ziegler, Phys. Rev. A 15, 2042 (1977).

[51] E. Kyrölä and S. Stenholm, Opt. Commun. 30, 37 (1979).

[52] E. Kyrölä and R. Salomaa, Appl. Phys. (Germany) 20, 339 (1979).

[53] E. Kyrölä and R. Salomaa, Phys. Rev. A 23, 1874 (1981).

[54] J. H. Shirley, Phys. Rev. 138, B979 (1965).

[55] S. Feneuille, J. Phys. B 7, 1981 (1974).

[56] S. Feneuille, M.-G. Schweighofer, and G. Oliver, J. Phys. B 9, 2003 (1976).

[57] A. M. Bonch-Bruevich, T. A. Vartanyan, and N. A. Chigir, Zh. Eksp. Teor. Fiz. 77, 1899 (1974) [Sov. Phys.—JETP 50, 901 (1979)].

[58] S. P. Goreslavskii and V. P. Krainov, Opt. Spektrosk. 47, 825 (1979) [Opt. Spectrosc. (USSR) 47, 457 (1979)]; S. P. Goreslavskii, N. B. Delone and V. P. Krainov, J. Phys. B 13, 2659 (1980).

[59] S. Geltman, Phys. Lett. A81, 27 (1981).

[60] For a general survey of coherent transient effects see Refs. 1–6; R. Shoemaker, in *Laser and Coherence Spectroscopy,* edited by J. I. Steinfeld (Plenum, New York, 1978), p. 197; and R. G. Brewer, Physics Today 30, 50 (1977).

[61] F. Rohart, P. Glorieux, and B. Macke, J. Phys. B 10, 3835 (1977); N. C. Wong, S. S. Kano, and R. G. Brewer, Phys. Rev. A 21, 260 (1980).

[62] D. Grischkowsky, Phys. Rev. A 7, 2096 (1973).

[63] D. Grischkowsky, M. M. T. Loy, and P. F. Liao, Phys. Rev. A 12, 2514 (1975).

[64] R. G. Brewer and E. L. Hahn, Phys. Rev. A 11, 1641 (1975).

[65] M. Sargent III and P. Horwitz, Phys. Rev. A 13, 1962 (1976).

[66] D. P. Hodginson and J. S. Briggs, Opt. Commun. 22, 45 (1977).

[67] J. R. Ackerhalt and B. W. Shore, Phys. Rev. A 16, 277 (1977); B. W. Shore and J. R. Ackerhalt, Phys. Rev. A 15, 1640 (1977).

[68] M. Ducloy, J. R. R. Leite, and M. S. Feld, Phys. Rev. A 17, 623 (1978); M. Ducloy and M. S. Feld, in Ref. 1, p. 243; J. R. R. Leite, R. L. Sheffield, M. Ducloy, R. D. Sharma, and M. S. Feld, Phys. Rev. A 14, 1151 (1976); M. S. Feld in Ref. 6, p. 203.

[69] M. P. Silverman, S. Haroche, and M. Gross, Phys. Rev. A 18, 1507 (1978).

[70] T. W. Mossberg, R. Kachru, S. R. Hartmann, and A. M. Flusberg, Phys. Rev. A 20, 1976 (1979), and references therein.

[71] A. Schenzle and R. G. Brewer, Phys. Rev. A 14, 1756 (1976); Phys. Rep. 43, 455 (1978).

[72] L. Kancheva, D. Pushkarov, and S. Rashev, J. Phys. B 14, 573 (1981).